TECHNICAL AND VOCATIONAL TRAINING INSTITUTE (TVTI)

School of Graduate Studies

FACULTY OF ELECTRICAL AND ELECTRONICS TECHNOLOGY AND INFORMATION AND COMMUNICATION TECHNOLOGY (DEPARTMENT OF ELECTRICAL AND ELECTRONICS TECHNOLOGY)

Field Oriented Control based Speed Control of Permanent Magnet Synchronous Motor using Higher Order Sliding Mode Controller

MSc Thesis for the Partial Fulfillment of

Master of Science in Electrical Automation and Control Technology Management

By,

Tola Negesa Mergo (MTR/761/13)

Supervisor,

Dr. Dereje Shiferaw

August, 2022

Addis Ababa, Ethiopia

Field Oriented Control based Speed Control of Permanent Magnet Synchronous Motor using Higher Order Sliding Mode Controller

A Thesis submitted to

TECHNICAL AND VOCATIONAL TRAINING INSTITUTE (TVTI)
FACULTY OF ELECTRICAL AND ELECTRONICS TECHNOLOGY AND INFORMATION AND COMMUNICATION TECHNOLOGY (DEPARTMENT OF ELECTRICAL AND ELECTRONICS TECHNOLOGY)

In partial fulfillment for the Degree

MASTER OF SCIENCE *in* ELECTRICAL AUTOMATION AND CONTROL TECHNOLOGY MANAGEMENT

By,

Tola Negesa Mergo (MTR/761/13)

Supervisor,

Dr Dereje Shiferaw

DECLARATION

Here by I declare that, this written thesis on field oriented control based speed control of permanent magnet synchronous motor using higher order sliding mode control is my unique work of my own, takes not yet presented for a masters thesis in this or other universities and all soursesof materials used for this thesis work have been fully acknowledged.

Name: Tola Negesa Mergo (MTR/761/13)

Signature: _____

Place: Addis Ababa

Date of Submission: _____

This thesis has been submitted for examination with my approval as a TVTI advisor.

Dr. Dereje Shiferaw _____

Advisor Name Signature Date

TECHNICAL AND VOCATIONAL TRAINING INSTITUTE (TVTI)
FACULTY OF ELECTRICAL AND ELECTRONICS TECHNOLOGY AND
INFORMATION AND COMMUNICATION TECHNOLOGY
(DEPARTMENT OF ELECTRICAL AND ELECTRONICS TECHNOLOGY)

Thesis on

Field Oriented Control Based Speed Control of Permanent Magnet Synchronous Motor Using Higher Order Sliding Mode Controller

By,

Tola Negesa Mergo (MTR/761/13)

APPROVED BY THESIS ADVISOR COMMITTEE

Name of the Advisor	Signature	Date
Dr. Dereje Shiferaw		02/09/2022
Name of Examiner Internal	Signature	Date
Dr.Petchinathan Govindan		02-09-2022
Name of Examiner, Internal	Signature	Date
Mr.Tesfaye Nafo		Sep 1/2022
Name of Examiner, External	Signature	Date
Dr. Bisrat Gezahegn		30/8/2022
Name of Chairperson	Signature	Date
Zemenu Tamir		02/09/22

ACKNOWLEDGEMENT

First and foremost, we would like to express our deep whole hearted gratitude to my advisor Dr. Dereje Shiferaw for sharing his unreserved skill, information, and experience. Without his committed support, this work would have been completed. His advice and support thesis cannot be done.

I am also thankful to Workineh Geleta for helping optimistically. To justify it, it is beyond a word to explain the way he guides me , the way he shares me his experience that couldn't be explained only imprinted in my mind. My appreciation also extends to my wife ,my parents and relatives who support and encourage me to complete this thesis in particular and the society in general.

ABSTRACT

In a range of industrial applications, permanent magnet synchronous motors (PMSM) have lately gained popularity in high-performance variable-speed drives. The great efficiency, compactness, high torque to inertia ratio, quick dynamic response, control, and maintenance-free operation of the PMSM are some of its many qualities. A PMSM's dynamic model is highly nonlinear due to the connection in between electrical values and the motor speed.

Variable voltage and variable frequency operation must be carried out to achieve high-performance dynamic on PMSM both actual location within the rotor. To do this, stator current and rotational speed must be measured mechanically and fed back to the controllers. Numerous loading scenarios will be taken into account in the performance study. An established technique for resolving nonlinear system control issues is sliding mode control. It is possible to provide characteristics of robustness to a variety uncertainty of, includes load torque disturbances and parameter perturbations. Traditional sliding mode controllers, however, suffer from a number of drawbacks, including chattering. In this thesis, higher order sliding mode control of speed techniques for PMSM are thoroughly examined.To explore the issue, the controller is evaluated using simulation with reference speeds and load fluctuation using Matlab/Simulink. To manage the torque and flux and to streamline system control, the motor is operated using field oriented control (FOC). The results of the simulation demonstrate that the load torque and parameter changes have no effect on the suggested drive's speed response. The developed controller functions effectively even after changing the reference speed, proving that the features of the reference speed have no bearing on speed regulation. The impact of chattering on the system is reduced, the speed response has a maximum, an In a steady state reaction, speed error is zero. overshoot of 1.531%, rise time 3.175ms, and settling time 1.926ms, according to the simulation result of comparation table 5.1 HOSMC is best because 32.32% (percent) to reduced chattering.

Keywords*: PMSM, FOC, HOSMC, PI, SVPWM, SMC, Chattering effect.*

TABLE OF CONTENTS

LIST OF FIGURES

LIST OF TABLE

ABBREVIATIONS

CLFO	Closed-Loop Flux
DC	Direct Current
DSP	Digital Signal Processor
DTC	Direct Torque Control
EMF	Electromotive Force
FOC	Field Oriented Control
IM	Induction Motor
LPF	Low Pass Filter
LTID	Load Torque Identification
MIMO	Multiple-Input, Multiple-Output
MTPA	Maximum Torque Per Ampere
N.D.	Negative-Definite
N.S.D.	Negative Semi-Definite
P.D.	Positive-Definite
PI	Proportional Integral
PLL	Phase-Locked Loop
PMSM	Permanent Magnet Synchronous Motor
PWM	Pulse Width Modulation
RPM	Round Per Minute
Sat	Saturation Function
Sgn	Sign Function
SMO	Sliding Mode Observer
SPMSM	Surface Mounted Permanent Sagnet synchronous motor
SVM	Space Vector Modulation
VSI	Voltage Source Inverter

CHAPTER ONE
INTRODUTION

1.1 Back ground

PMSMs are frequently used in high-performance drives and low- to mid-power applications, such as robotics, electric vehicles, and machine tools. They are gradually replacing induction motors in many application fields due to advantages including compact structures, high air-gap flux density, high power density, high torque to inertia ratio, and high efficiency. Time-varying parameters with complex high-order dynamics make up nonlinear PMSM systems. Outstanding performance [1].

Accurate rotor position of PMSM for fast dynamic response is required for field-oriented control, which is typically provided through a shaft-mounted optical encoder, resolver, or Hall sensors. However, it is extremely desirable to eliminate such sensors in order to save money, mount space, and increase mechanical robustness and system reliability, which are critical in many applications [2]. For rapid four-quadrant operation, good acceleration, and a smooth start, PMSM drives are designed with field-oriented control, also known as vector control. On the other hand, high-performance controlling need precise details of the rotor position. This is it can be accomplished by utilizing position sensors such as resolvers, tachometers, and encoders. The PMSM's rotor speed and position are precisely measured by this mechanical sensor, despite the fact that it increases the size of the device. Contrarily, the PMSM is a multivariable coupled system with a high level of nonlinearity. and its performance is impacted by changes in the plant's parameters, unmodeled nonlinear dynamics, and external load disturbances[3].

Some robust control systems, There have been created Sliding mode, adaptive control, and nonlinear control controls (SMC) to achieve good dynamic response. As a result of the fast dynamic, reaction and is not affected to an outside load disturbances furthermore, a parameter fluctuations in the SMC a potent nonlinear control approach that been extensively used employed for PMSM position and speed control. In addition, the proper sliding surface for the control system can be chosen to reduce order. Typically, the design of a PMSM's sliding surface is restricted to differentiating or integrating the state variables in integer order. The

control system's high frequency oscillations, however, brings about the chattering phenomenon of sliding mode control [4].

1.2 Statement of the problem

In a range of industrial applications, permanent magnet synchronous motors (PMSM) have lately gained popularity in high-performance variable-speed drives. The rapid dynamic response, high torque to inertia ratio, and efficiency, straightforward maintenance-free operation, modeling, and control are only a few of the PMSM's many properties that account for this. The dynamic version of a PMSM isvery nonlinear due to the connection between the electrical values and the motor speed. Variable voltage and variable frequency operation must be carried out to acquire excessive dynamic overall performance on PMSM and real function of the rotor. To do this, stator current and rotational speed must be measured mechanically and fed back to the controllers. An established technique for resolving nonlinear system control issues is sliding mode control. It is possible to provide characteristics of robustness to a variety of uncertainties, including Torque disturbances caused by load and parameter variations. However, traditional sliding mode controllers have several dis advantages, such as chattering. Therefore to solve the problem of a SMC, this thesis focuses on applying higher order sliding mode controller. This thesis proposed a comprehensive study of the higher order sliding mode methods of speed control for PMSM, which can assure robustness against a load torque disturbance and parameter variation with chattering reduction.

1.3 Objective

1.3.1 General Objective

The main objective of this thesis is to model, design and simulate FOC based speed control of permanent magnet synchronous motor using higher order sliding mode controller.

1.3.2 Specific Objective

This study seeks to develop a system that will address the following:

- To adapt mathematical model of permanent magnet synchronous motor
- To design High Order Sliding Mode Controller for PMSM Speed Control
- To analyze the performance of HOSM controller under various loading conditions.
- To carry out simulation tests of the proposed HOSMC control and compare these to other conventional SMC control schemes.
- To simulate the system using Matlab/Simulink

1.4 Methodology

For a class of MIMO nonlinear systems, a higher order sliding mode controller is proposed. The controller synthesis takes three methodologies to HOSM controller-based speed control of PMSM.

a) The higher order sliding mode problem is expressed in terms of input-output;
b) By considering uncertain nonlinear functions as bounded nonstructured parametric uncertainties, the problem is viewed in an uncertain linear context.
c) A time varying manifold is designed using the optimal sliding-mode design for linear systems by minimizing a quadratic cost function over a finite time interval with a fixed final state.

The design and testing of a controller for a permanent magnet synchronous motor shows that the controller is well suited for simulation and that the gain of the controller can be synthesized using all the features of linear quadratic control.

1.5 Scope the study

The purpose of this thesis is to propose a more straightforward method for better PMSM control even with unknown system dynamics, thus overcoming the aforementioned shortcomings and system complexity. The control gains in vector control are calculated solely based on the motor power ratings. With the aid of a PI controller, precise tracking of the PMSM's speed and d-q axis currents is seen. The findings demonstrate accurate tracking of the currents and speed. Subsequently, various novel PMSMs are simulated using these generalized mathematical expressions to validate this proposed controller HOSMC.

The influence of PMSM modeling equations on the d-q axis currents and speed control tracking are used in the condensed control scheme. For each of the SMC controller gains, substantially simpler mathematical formulas are obtained in this case compared to the vector control. The Matlab/Simulink environment is used for all simulations, and conclusions are drawn in response.

1.6 Limitation of the study

This thesis aims to simulate and construct the speed control of a permanent magnet synchronous motor that makes use of a mechanical position/speed sensor to measure the rotor's instantaneous mechanical position/speed.

Table 1.1 System limitations and assumptions

Component	Description of the limitation, assumptions
System	Is symmetric and balanced
VSI	Generates the voltage perfectly from the duty cycles
Magnetic core	Magnetic saturation limits are not reached
Machine electric losses	Such as core losses, Eddy current losses etc are neglectable
Motor parameters	Are constant as well as the device temperature
Sampling frequency of the system	5 kHz
Switching frequency of the VSI	5 kHz

1.7 Significance of the sudy

This thesis applies the research of nonlinear control and high order sliding mode control theory in PMSM control, and achieves robust control for a PMSM in spite of the internal parameter uncertainties and unknown external disturbance load torque. In addition, the estimation online of system state variables is also one of the hot issues in the control field. In this thesis, a new design based on high order sliding mode with differentiator for PMSM, access to the state variable estimation; Besides, unknown uncertain load impacts the performance of motor control. In order to improve system performance, also achieves external disturbance load estimation online. It makes sure the load can be accurately estimated.

1.8 Research Outline

This thesis is divided in Six chapters. The 1st chapter provides an overview of the PMSM speed control using the HOSM controller, including the Background information on PMSM speed control, a problem definition, significance, collect more information, methodology, scope, and limitations of the study. In chapter two, the various control theory techniques of the PMSM are presented, and various literatures related to speed control of PMSMs are reviewed. The third chapter discusses system modeling, design, analysis, and implementation.

The fourth chapter describes the standardized controller method, as well as the controller and observer tuning processes. Chapter five presents and discusses simulation results. The thesis

work's contributions are covered in the same chapter as well. Chapter six concludes with recommendations and presented.

.

CHAPTER TWO

LITERATURE REVIEW

A synchronous motor known as a permanent magnet synchronous motor (PMSM) creates the air gap magnetic field using permanent magnets for the rotor instead of electromagnets. The stator is multiphase, and in a steady state, the electrical frequency of the stator is directly proportional to the rotor speed. It's different from a conventional synchronized device though that it, in eliminates rotor conductors and instead uses the field winding in place of permanent magnets. The rotor has permanent magnets increase effectiveness do away with requirement as well as slip rings do away with complex the dynamics of electrical rotors, in particular the outer windings of the permanent magnet rotor with type of motor have several advantages over other types, including low inertia of the rotor effective dispersion of heat, smaller sized motor, compact and increased power density, no spark, despite strong air-gap flux during change and high efficiency [5].

In 2007 Marek Stulrajter, Val´eria Hrabovcov´a and Marek Franko [6] presents many methods for PMSM control legislation. As potential techniques for controlling AC motors, scalar and vector control were chosen.The properties of these control techniques are briefly described in the theoretical background. Simulations highlight and confirm several advantages and disadvantages. The paper demonstrated the use scalar controls have the advantage of sensor-less operation. However, Scalar control does not work in an open loop.work since it allow for current control, PMSM behaves differently during various operation cycles such as startup and loading.

In 2011 Cunjian Xia, Xiaocui Wang, Shihua Li and Xisong Chen[7] Techniques for 2011 to Improve the Disturbance Rejection Property of Integral Sliding Mode Speed Control for PMSM System a speed control system for permanent magnet synchronous motors (PMSM). However, the results of the simulation and implementation display that balancing anti-disturbanceandchatteringcapabilitiesisdifficult.Three types of superior ISMCmanipulate tech niques are being advanced to that end. First, an ISMC with linearly various benefit is created. Usingthisapproach,theISMCcontroller'sswitchinggainmay be decreased evenas nevertheless making sure thatthe speed.areachesits consistent unitedstates andasa endresult reducing const ant usa fluctuations.Furthermore,thePMSMsystem'santidisturbance performance mayaddition

ally beguaranteed.Second,an imperative slidingmode manipulate isdeveloped using an prolon ged nation observer (ESO). ESO can estimate both states and disturbances at the same time. ESO is used to obtain an estimate of the lumped disturbances, which is then used in the the composite ISMC control law's feed forward compensation design. Specifically, the controller can set the switching gain to a lower value without sacrificing disturbance rejection performance, which helps to reduce large chattering caused by high control gains. Third, to take advantage of both improved methods A linear changing gain and ESO adaptive composite control system is created. The advantages of these upgraded techniques can be seen in their ability to reduce chattering while retaining dynamics and interruption minimization capabilities. both experimentation and simulations findings are given. However, the proposed article lessens chattering but does not completely do away with it. Chattering is eliminated in higher order sliding modes by moving discrete elements to higher derivatives of output variables.

In 2011 Mahlet Legesse Gebresilassie [8] emphasizes on a Permanent Magnet Synchronous Motor's ability to control speed (PMSM). a controller that uses proportional-integral (PI) frequently utilized Despite the fact that a PMSM, requires other contemporary control not linear approaches. On the other hand, Speed variations, load disturbance, and other factors might cause PI controllers to malfunction. parameter variations if its gains are not continuously tuned. The conventional method for solving these problems is to observe the system reaction and manually adjust the proportional and integral gains. The PI settings must be modified online and automatically to minimize tiresome duties manually controlled. Although the respected Ziegler-Nichols approach for adjusting PI controller coefficients is fairly straightforward, it does not necessarily ensure effectiveness. This thesis suggested creating an online self-tuning PI controller method based on a fuzzy logic controller as a consequence (FLC).Througsimulationutilizing the Real Time Workshop (RTW) Matlab/Simulink software packaging, the efficiency of the suggested a controller assessed for a varied variety referencing speeds and load variations. The thesis here says an FLC with 49 rule is suggested to enhance the drive system's performance that is dynamic. The simulation results demonstrate that adjustments in load torque and parameters have no impact on the proposed drive's speed response. Additionally, the developed controller performs admirably regardless of the reference speed being altered, demonstrating that is reference speed's characteristics have no

bearing on the developed controller's ability to regulate speed. These show a notable performance enhancement over traditional PI speed controllers. The architecture in this study is kept straightforward, although torque and flux control are handled by the PI controller. Performance consequently decreases to some extent. Therefore, a PID controller is employed for torque and flux control in order to increase performance.

In 2010 Huangfu Yigeng1, S. Laghrouche, Liu Weiguo1 and A. Miraoui [9] uses high order sliding mode control theory and nonlinear control to PMSM control to achieve reliable control despite Unknowns involving internal parameters and unidentified external influences. perturbation load torque. Additionally, online estimation of system state variables is a hot topic in the control industry. The simulation results demonstrate good performance. In addition to providing access to state variable estimation and a new design for PMSM using a differentiator for high order sliding mode this work also discusses the impact of unknown uncertain load on motor control performance. To enhance performance of the system work uses realtime burden from external disturbances calculation. Synchronous motors consistently outperform in both dynamic performance and steady accuracy in experiments and simulations, proving the viability of this technology in real-world systems. High order sliding mode control, which maintains the robustness of conventional sliding mode control, also validates this technology. The high order sliding mode substantially reduces the chattering caused by discrete control rules. In a different way, the simulation give future control for nonlinear systems with high order sliding mode applications a certain reference value. This document illustrates how to control the motor's position and demonstrates the benefit of the HOSM controller. However, the paper also uses input/output feedback linearization and a differentiator. The system grows more intricate as a result. As a result, I decreased the chattering impact and simplified the system architecture in my thesis.

In 2014 Zhugang Ding, Guoliang Wei and XuemingDing [10], permanent magnet synchronous motor (PMSM) speed identification and control problem for sliding mode are addressed concurrently. As a result, an MRAS speed observer with a changeable structure is created to do away with the requirement for the sensor is mechanical. Instead of the traditional signum function, In variable-structure control, a sigmoid purpose with a programmable improvement is utilized as analoggous control. to reduce system chattering. Second, a sliding mode controller replaces the conventional speed PI actuator. To some extent, it compensates

for the shortcomings of the speed PI regulator. Lastly, the simulation result validated the method's reasonability and reliability. The simulation results show that when the reference speed and load torque change, this speed observer can track it quickly and precisely, and the three-phase current and torque of the motor have a good dynamic response. Clearly, simulation results show that the proposed control scheme eliminates speed overshooting while also providing fast reaction and powerful robustness. This does not reduce chattering, because removing the mechanical sensor causes to system instability because obtaining accurate rotor position from the observer is difficult.

In 2010 Marwa Ezzat, Nicolas Gonzalez and Alain Glumineau [11] presentes an Observer-Controller Scheme for Sensorless Speed Control of Permanent Magnet Synchronous Motors Using High Order Sliding Mode Techniques. This paper makes use of immoderate order slidingmode techniques to clear up the pace manipulate trouble for a sensorless eternal magnet synchronous motor (PMSM). An observer is created the use of a exceptional twisting set of guidelines todeterminethemotor'slocationandspeedinparticular based completely on moder n and voltage measurements. Under the presence of parameter uncertainties, a quasi-non-stop excessive orderslidingmodecontrollerisdesignedto music the pace of a favored reference. To disclose the usual performance oftheproposedscheme,simulation effects are provided with inside the context of an business benchmark. The effects are obtained no be counted unknown parameter uncertainties in stator resistance and inductance. In addition, the Using a business benchmark, the system (an observer-based controller and motor) is evaluated. Simulated findings show that the proposed sensorless observer controller scheme passes thorough robustness tests is efficient. Even if this research eliminates the chattering issue, does not guarantee system stability due to the observer's accuracy on rotor position. The system design is also more complicated as a result of the use of input output feedback linearization. To simplify the system to regulate the currents, a PID controller should be used..

In 2010 Yi-Geng Huangfu [12] prestes research on nonlinear systems, In 2010, PMSM added high order sliding mode control and related features Since of its inherent benefits the paper focuses greater on the PMSM. This work integrated successful MIMO nonlinear high order sliding mode control of a permanent magnet synchronous motor research to enhance performance. Instead of close to equilibrium point linearization, it converts the coupling nonlinear PMSM into a controlling a linear subsystem with a single input and single output

(SISO).The nonlinear and coupling issue for PMSM has been resolved as a result. Additionally, the technique for nonlinear uncertainty has drawn a lot of attention. Because the effective deployment of strong controls actually sacrifices some performance. The closed loop bandwidth is usually constrained by this type of robust control method. lowering the robustness and performance of the system under monitor. Sliding mode control is hence a useful technique for enhancing system resiliency. The first section of this thesis made a sound recommendation for a for PMSM, a high order sliding mode controller. The device provides correct accuracy of location servo tracking despite parameter uncertainty and an outside torque disturbance. The simulation's results demonstrate that the look at fee has a high degree of when the differentials of the sliding mode variable are precise converge to zero. the online calculation of unknown outside torque disturbances for PMSM employs a similar concept. As if, load torque won't be a mysterious disturbance any longer. Performance of the system can be considerably enhanced. It establishes the theoretical foundation for upcoming applications. The paper's conclusion includes a hardware experiment implementation. The findings of the studies demonstrate that PMSM can achieve With an excellent dynamic and steady character, the system servo tracking control employing valuable feedback linearization decoupling and a high order sliding mode controller. High order sliding mode control technology, in contrast to conventional sliding mode control, transfers the chattering phenomena produced higher order sliding surface in discontinuous discrete control, reducing chattering and enhancing control precision. This work focuses on high order sliding mode control for nonlinear control, and position tracking to increase overall system performance when all of the aforementioned factors are taken into account, however when we look at the whole system architecture, it is more complex and not cost-effective.

In 2014 Romain Delpoux Thierry Floquet [13] presented on High order sliding mode control for sensorless trajectory tracking of a PMSM. The paper presents a new sensorless approach for permanent magnet synchronous motor (PMSM). Current sensors are assumed available, but position and velocity sensors are not. Based on the electrical equations, sliding mode observers are designed to estimate the back-EMF of the motor. These estimations are used to reconstruct the position and the velocity. From this estimation, a robust sliding mode control is developed which ensures the position tracking of the motor. A new reference frame is used that presents advantages similar to the standard (d−q) frame, but without the need for a position

sensor. The efficiency of the algorithm is shown through experimental results. Making a sensorless cause instability of a system because it is very difficult to get the accurate position of the rotor. In this thesis, after the analysis/investigation, review and comparison of several speed controls of PMSM techniques, a combination of higher order siding mode controller and PI controller is used. Because it reduces/eliminates the chattering effect, makes the system robust under parameter variation and load torque disturbance, gives a quick dynamic response, eliminates the basic steady-state error, makes the system design simple and stable.

Xiaoguang Zhang, Lizhi Sun, Ke Zhao, and Li Sun, [14] In order to optimize the speed-control performance of the permanent-magnet synchronous motor (PMSM) system with different disturbances and uncertainties, a nonlinear speed-control algorithm for the PMSM servo systems using sliding-mode control and disturbance compensation techniques is developed in this paper. First, a sliding-mode control method based on one novel sliding-mode reaching law (SMRL) is presented. This SMRL can dynamically adapt to the variations of the controlled system, which allows chattering reduction on control input while maintaining high tracking performance of the controller. Then, an extended sliding-mode disturbance observer is proposed to estimate lumped uncertainties directly, to compensate strong disturbances and achieve high servo precisions. Simulation and experimental results both show the validity of the proposed control approach.a new procedure for controlling speed and estimating load torque was introduced.

Zhuang Xu and M. F. Rahman, [15] The estimation accuracy of the stator flux and speed using open-loop integrators drops as the mechanical speed reduces in direct-torque-controlled (DTC) interior-permanent magnet (IPM) synchronous motors. At lower speed, inaccurately estimated stator flux and stator resistance mismatch have significant influence on the steady-state and transient performance of the drive system. The robustness against parameter detuning and signal noises can be improved by deploying closed-loop observers with estimated stator flux and rotor speed. This paper presents a comparison of two stator-flux and speed observers for variable-structure DTC IPM motor drives: an adaptive sliding observer and an extended Kalman filter (EKF). The experimental comparison of the adaptive sliding observer and the EKF regards steady-state and dynamic performance, robustness against parameter uncertainties, stability, and computational complexity. Recommendations for observer

selection and the effectiveness of the various schemes are concluded. investigated the direct-torque estimation performance of a sliding observer versus a Kalman filter.

In 2017 Elhangari, Abdelbaset [16] The control objective is to track a reference speed with the actual speed of rotor. In order to achieve the desired speed, the phase voltage must be varied as a function of rotor angular displacement. The angular speed of the synchronous motor depends on the frequency of the voltage applied to the stator windings. This neccesitates the measurement of angular displacement of the motor. The error signal between the reference and actual speeds represents the sliding surface s. The sliding mode controller is derived from the d-q variables and is based on Lyapunov's stability concept. Moreover with the addition of an observer to estimate the applied load torque, it can compensate for load torque disturbances. Hence the torque ripples get reduced in Permanent Magnet Synchronous Motor. The results obtained in Sliding Mode Control is compared with the conventional Direct Torque Control..

In 2013 Michael Ruderman, Alex Ruderman, and Torsten Bertram [17], The impact of additive periodic torque disturbances on the controlled motion of permanent magnet motors can be significant. The paper shows how an observer-based drive control can efficiently reject the harmonic torque disturbances providing smooth angular velocity. The proposed control design is based on the state-space torque harmonics representation and Luenberger observer that proved to be adequate. The designed control algorithms are verified using an experimental setup with a permanent magnet synchronous motor with well-detectable torque harmonics. The rejection of additive position periodic torque disturbances is experimentally demonstrated for two first harmonics and that for different angular velocities. an observer-based terminal Sliding-Mode control method is used to regulate the speed of the PMSM with load torque. Some of these controllers use a speed sensor, while others do not. A sliding-mode observer was used.

In 2011 Hongryel Kim, Jubum Son, and Jangmyung Lee, [18] In order to apply a sensorless PMSM control which is robust against parameter fluctuations and disturbances, a high-speed SMO is proposed, which estimates the rotor position and the angular velocity from the back EMF. In the conventional SMO, a low-pass filter and an additional position compensation of the rotor are used to reduce the chattering problem that is commonly found in the SMO using the signum function. In order to overcome the time delay caused by the low-pass filter, in this research, a sigmoid function is used for the switching function instead of the signum function.

Also, the variation in the stator resistance is estimated to improve the steady-state performance of the SMO. The stability of the proposed SMO was verified using the Lyapunov second method to determine the observer gain. The validity of the proposed high-speed PMSM sensorless velocity control has been demonstrated with simulations and real experiments. To estimate load disturbances for a high-speed permanent magnet synchronous motor.

2.1 Summary of Literature Review

In this chapter, the theory of variable structure control has been skimmed. HOSMC may be preferably designed to manage linear or nonlinear systems with unknown dynamics because it demonstrates several advantages. The selection of the sliding parameters and the estimation of the bounding functions of the unknown components have a significant impact on the system performance and control quality, even though resilience can be achieved without exact knowledge of the control system.

This thesis uses speed control of PMSM a mix of a higher order siding mode controller and a conventional sliding mode controller for studying, researching, evaluating, and comparing various speed controls of PMSM approaches. Because it significantly lowers or reduces chattering and improves the system resistant to variations in the parameters and load torque disturbance, provides a rapid dynamic responseremoves the fundamental continuous-state error, and simplifies and stabilizes the system design.

CHAPTER THREE

MODELING AND DESIGNING OF A SPEED CONTROL OF PMSM

3.1 Introduction

In comparison to induction motors, permanent magnet synchronous motor drives (PMSM) have a number of advantages, such as improved overall efficiency, better utilization of reluctance torque, lower losses, and a smaller motor size. The field oriented control has been acknowledged as a feasible and robust option to meet these needs. Numerous studies have been undertaken in recent years to identify various solutions for the PMSM drive control that have the qualities of quick and precise torque response. This chapter covers the precise mathematical modeling of a PMSM and controller design refers to permanent magnet synchronous motors. The discussion is on the field-oriented regulation in of the motor regions of constant weakening of torque and flux The inner loop is constructed using a PI controller to regulate the flux and torque generated by the motor, while A controller with higher order sliding mode (HOSM) is used to produce the outer loop and regulate the motor speed. The next sections include illustrations and a brief overview of the speed controller design as well as different control design components such SVPWM, inverters, and speed/position sensors. The model is used to simulate the field oriented control (FOC) system in the MATLAB/ SIMULINK environment.

3.2 Mathematical Model of PMSM

The PMSM is surprisingly similar to a normal wound rotor synchronous machine, with the distinction of not having damper windings and being powered by a field winding as opposed to a permanent magnet. The equations for damper windings and field current dynamics can be removed as a result, and the well-known synchronous machine model can be used to construct the d, q model of the PMSM.

3.2.1 Reference Frame Transformation

To obtain the time-varying values of the motor parameters, the a PMSM's stator reference frame is transformed into a reference frame for a rotor. FOC measures the variables iq and id in the rotating frame of reference. stator current measurements must first be converted from the reference frame for the three phase d-q rotor rotating on two axes time variation stator reference frame. Vector projection is used to perform a reference frame transformation. The given f vector is first rotated by the α angle. Vector v is now aligned with the x-axis, and

vector f is placed γ, α degrees from the axis. The projected vector is obtained in the final step by taking the real part of the vector. The detailed derivation of these equations from abc-reference to dq-reference will be:

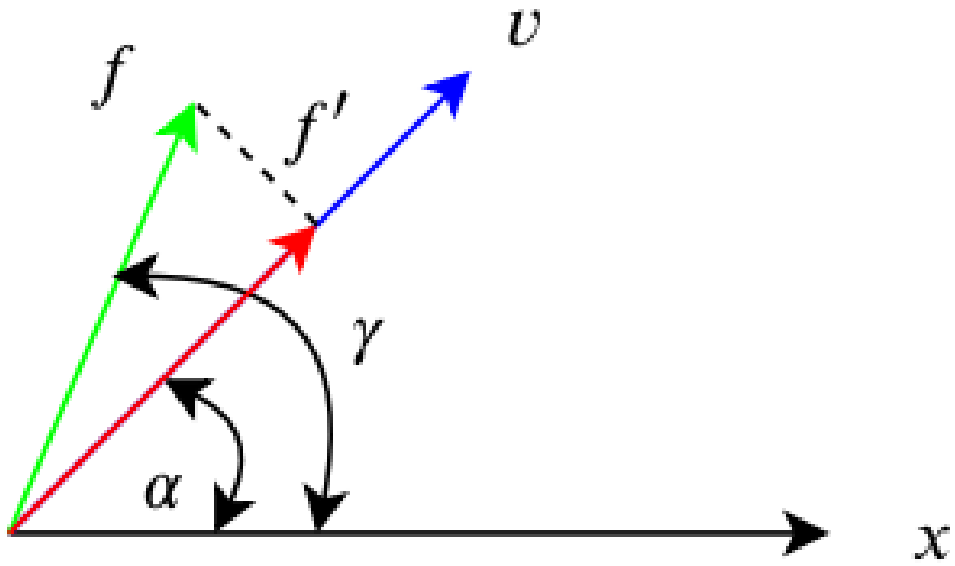

Figure 3.1 Arbitrary vectors for vector projection [8]

Vector projection equation will be:

$$f' = R_e\left(\frac{f}{e^{j\alpha}}\right) \tag{3.1}$$

Where the real part of the expressions are taken by forming the complex conjugate of the given f vector, denoted as f'.

$$R_e(f) = \frac{f + f^-}{2} \tag{3.2}$$

This transformation is performed primarily to reduce complexity when working with differential equations and to eliminate time-varying components. When deriving the voltage equation from stationary abc to rotating dq-reference frame transformation, the following method is used. Because it allows the motor variables to be seen as constant values, the rotating dq-reference frame is used to describe the differential equations of the motor [18]

Vector in the abc reference frame is given

$$\bar{f}_{abc} = \frac{2}{3}\left(f_a e^{j0^o} + f_b e^{j120^o} + f_c e^{-j120^o}\right) \tag{3.3}$$

Vector in dq reference frame is given by

$$f_{dq} = \left(f_d - f_q \right) e^{j\theta} \tag{3.4}$$

Where

θ is the angle between the two reference frame.

Since the system variables a, b, c are balanced or symmetrical, the zero component $f_0 = 0$, as shown in equation 3.5.

$$f_0 = \frac{1}{3}\left(f_a + f_b + f_c \right) = 0 \tag{3.5}$$

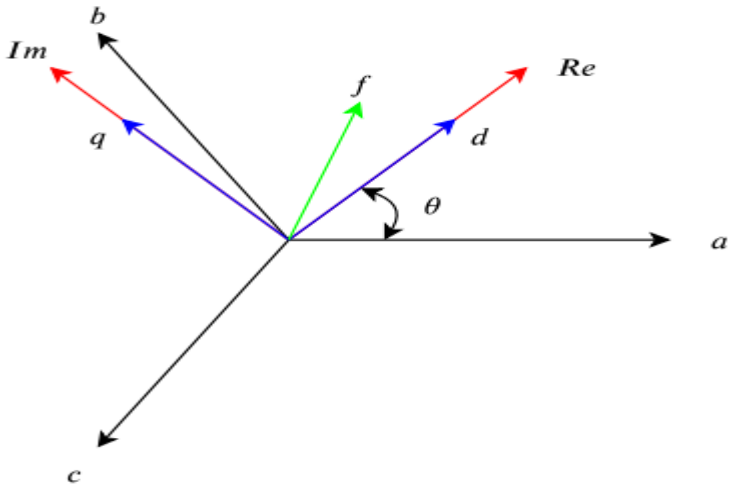

Figure 3.2 dq reference frame in the abc reference frame [8]

The q-axis is 90° ahead of the d-axis [19] and θ angle away from the a-axis, as shown in the figure. When the a-axis is used as the reference axis, the d and q components are as follows.

$$f_d = R_e\left(\frac{\bar{f}_{abc}}{e^{j\theta}} \right) = R_e\left(\frac{2}{3}\left(\frac{f_a e^{j0} + f_b e^{j120} + f_c e^{-j}}{e^{j\theta}} \right) \right)$$

$$= \frac{2}{3}\left(f_a \cos(\theta) + f_b \cos\left(\theta - 120^o\right) + f_c \cos\left(\theta + 120^o\right) \right) \tag{3.6}$$

$$f_q = R_e\left(\frac{\bar{f}_{abc}}{e^{j\theta + 90^o}} \right) = R_e\left(\frac{2}{3}\left(\frac{f_a e^{j0^o} + f_b e^{120^o} + f_c e^{-j120^o}}{e^{j\theta + 90^o}} \right) \right)$$

$$= \frac{2}{3}\left(-f_a \sin(\theta) - f_b \sin\left(\theta - 120^o\right) - f_c \sin\left(\theta + 120^o\right) \right) \tag{3.7}$$

As a result, the transformation matrix for the abc-to-dq transformation is equation 3.8.

$$\begin{bmatrix} f_d \\ f_q \\ f_0 \end{bmatrix} = K_{abc2dq} = \frac{2}{3}\begin{bmatrix} \cos(\theta) & \cos(\theta-120^o) & \cos(\theta+120^o) \\ -\sin(\theta) & -\sin(\theta-120^o) & -\sin(\theta+120^o) \\ \frac{1}{2} & \frac{1}{2} & \frac{1}{2} \end{bmatrix}\begin{bmatrix} f_a \\ f_b \\ f_c \end{bmatrix} \tag{3.8}$$

When this is substituted into the motor voltage differential equation 3.9, the following calculations are obtained.[20]

$$\begin{bmatrix} i_a \\ i_b \\ i_c \end{bmatrix} = \begin{bmatrix} R_s & 0 & 0 \\ 0 & R_s & 0 \\ 0 & 0 & R_s \end{bmatrix}\begin{bmatrix} i_a \\ i_b \\ i_c \end{bmatrix} + \frac{d}{dt}\begin{bmatrix} \lambda_a \\ \lambda_b \\ \lambda_c \end{bmatrix} \tag{3.9}$$

When equation (3.8) is multiplied by equation (3.9), the voltage equation in the dq-reference frame is obtained, (3.10)

$$\begin{bmatrix} i_a \\ i_b \\ i_c \end{bmatrix} = K_{abc2dq}\begin{bmatrix} R_s & 0 & 0 \\ 0 & R_s & 0 \\ 0 & 0 & R_s \end{bmatrix}\begin{bmatrix} i_a \\ i_b \\ i_c \end{bmatrix} + K_{abc2dq}\frac{d}{dt}\begin{bmatrix} \lambda_a \\ \lambda_b \\ \lambda_c \end{bmatrix}$$

$$= \begin{bmatrix} R_s & 0 & 0 \\ 0 & R_s & 0 \\ 0 & 0 & R_s \end{bmatrix}\begin{bmatrix} i_d \\ i_q \\ i_0 \end{bmatrix} + \frac{d}{dt}\begin{bmatrix} \lambda_d \\ \lambda_q \\ \lambda_0 \end{bmatrix} - \omega_r \begin{bmatrix} 0 & 1 & 0 \\ -1 & 0 & 0 \\ 0 & 0 & 0 \end{bmatrix}\begin{bmatrix} \lambda_d \\ \lambda_q \\ \lambda_0 \end{bmatrix} \tag{3.10}$$

The $\alpha\beta$ reference frame is perpendicular to the phase α a-axis, and the β -axis is 90° away from it.

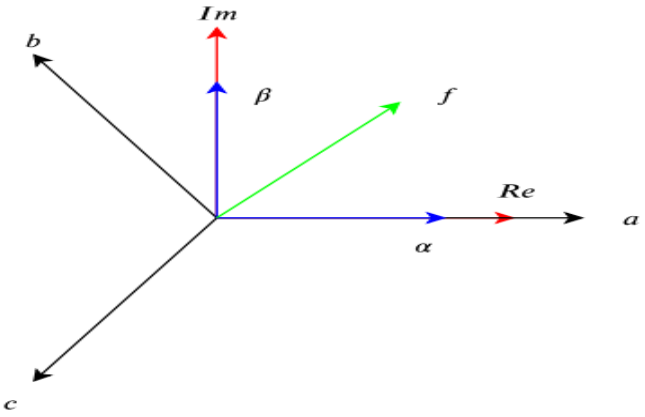

Figure 3.3 αβ reference frame in the abc reference frame [8]

The same calculations as shown above are performed with vector projection, yielding the following transformations matrix, equation (3.11).

$$\begin{bmatrix} f_\alpha \\ f_\beta \\ f_0 \end{bmatrix} = K_{dq2\alpha\beta} = \frac{2}{3}\begin{bmatrix} 1 & \cos(120^o) & \cos(-120^o) \\ 0 & \sin(120^o) & \sin(-120^o) \\ \frac{1}{2} & \frac{1}{2} & \frac{1}{2} \end{bmatrix}\begin{bmatrix} f_d \\ f_q \\ f_0 \end{bmatrix} \tag{3.11}$$

After that, the transformation matrix is multiplied by equation (3.10), yielding a voltage equation in the reference frame [21]. The machine inductance will be L_s.

$$L_d = L_q = L_s \tag{3.12}$$

The motor voltage zero term (v_0) is zero because the system is assumed to be symmetrical and balanced [22][23]

$$\begin{aligned} v_d &= R_s i_d + p\lambda_d - \omega\lambda_q \\ v_q &= R_s i_q + p\lambda_q + \omega\lambda_q \\ v_0 &= 0 \end{aligned} \tag{3.13}$$

For a non-salient pole machine, the machine flux-linkage is position dependent and the machine inductance is constant in the abc-reference frame; however, because the model has already been transformed into the *dq*-reference frame, the machine inductance is constant. The stator dq-reference frame is in sync with the rotor reference frame, which is also in sync. At no load, the rotor d-axis is chosen to be aligned with the maximum flux density line. The *q*-axis is always 90°electric ahead of the d-axis. This aligns it with the minimum flux density line [22] .

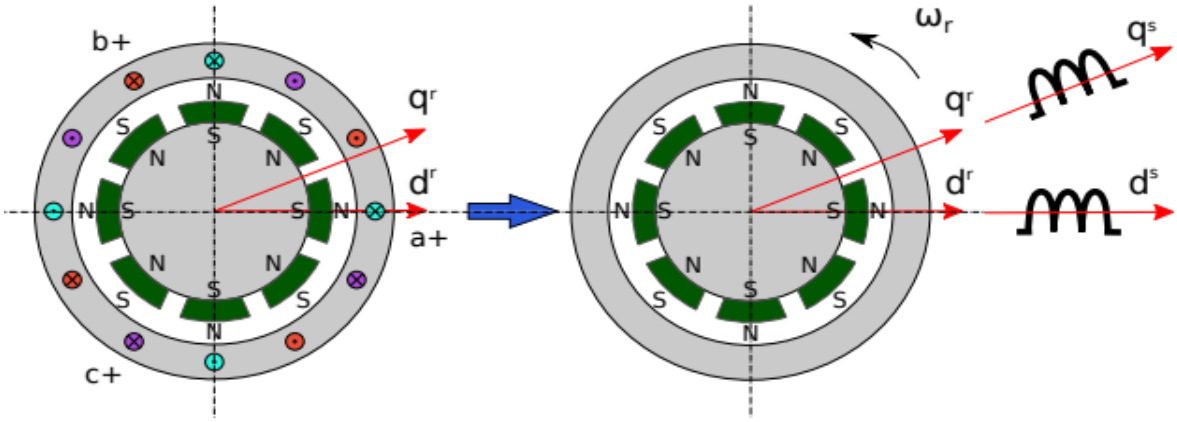

Figure 3.4 Stator Reference frame transformation from abc to dq [22]

The two d-axes are now parallel. This is useful because it produces the d-axis and q-axis flux-linkage shown in equation (3.14).

$$\begin{aligned}\lambda_d &= \left(L_{ls} + L_{md}\right) i_d + \lambda_{mpm} = L_d i_d + \lambda_{mpm} \\ \lambda_d &= \left(L_{ls} + L_{mq}\right) = L_q i_q \\ \lambda_0 &= 0\end{aligned} \tag{3.14}$$

The voltage equations can be rewritten after substitution, as shown in equation (3.15).

$$\begin{aligned}v_d &= R_s i_d + p\left(L_d i_d + \lambda_{mpm}\right) - \omega_r L_q i_q \\ v_q &= R_s i_q + p\left(L_q i_q\right) + \omega_r \left(L_d i_d + \lambda_{mpm}\right)\end{aligned} \tag{3.15}$$

Where p is the differential operator $\frac{d}{dt}$. Differentiating the equation, keeping in mind that the derivative of a constant is zero, will be the following results.[23]

$$\begin{aligned}v_d &= R_s i_d + L_d p i_d - \omega_r L_q i_q \\ v_q &= R_s i_q + L_q p i_q + \omega_r \left(L_d i_d + \lambda_{mpm}\right)\end{aligned} \tag{3.16}$$

The system's homogeneous first-order differential equation is obtained in a subsequent step.

$$\begin{aligned}\frac{d}{dt} i_d &= \frac{R_s}{L_d} i_d + \frac{1}{L_d} v_d + \omega_r \frac{L_q}{L_d} i_q \\ \frac{d}{dt} i_q &= \frac{R_s}{L_q} i_q + \frac{1}{L_q} v_q - \omega_r \frac{L_d}{L_q} i_d - \frac{1}{L_q} \omega_r \lambda_{mpm}\end{aligned} \tag{3.17}$$

Equations (3.15) also include the back-EMF voltage components, which are critical in position estimation and are highlighted here:

$$\begin{aligned}e_d &= -\omega_r L_q i_q \\ e_q &= \omega_r \left(L_d i_d + \lambda_{mpm}\right)\end{aligned} \tag{3.18}$$

The governing torque equation can be derived from the windings' input power equation[24]. Simplifying this equation with the PMSM machine's attributions results the following expression:

$$T_e = \frac{3}{2} N_{pp} \left(\lambda_d i_q - \lambda_q i_d\right) \tag{3.19}$$

$$T_e = \frac{3}{2} \frac{N_{poles}}{2} \left(\lambda_{mpm} i_q + \left(L_d - L_q\right) i_d i_q\right) \tag{3.20}$$

$$T_e = \frac{3}{2} N_{pp} \left(\lambda_{mpm} i_q\right) \tag{3.21}$$

The mechanical equation of the system can be derived using Newton's second law, as shown in equation (3.22).

$$T_e = J\frac{d\omega_m}{dt} + B_m\omega_m + T_{dist} \tag{3.22}$$

where J is the total system inertia, T_{dist} is the disturbance torque, consists of the load torque and coulomb friction.

The total system inertia includes the inertia of the IM and PMSM machines, as well as the coupling and fastening components that connect them. The first term refers to the torque required to accelerate the system without friction, while the last two terms refer to the torque required to overcome viscous friction and disturbance torque, respectively.

3.2.2 PMSM State Space Model

The state space form is developed using the machine's voltage equations expressed as first-order differential equations, as shown in equations (3.17).

$$\begin{aligned} \dot{x} &= Ax + Bu \\ y &= Cx \end{aligned} \tag{3.23}$$

$$\begin{bmatrix} i_d \\ i_q \end{bmatrix} = \begin{bmatrix} -\frac{R_s}{L} & \omega_r \\ -\omega_r & -\frac{R_s}{L} \end{bmatrix} \begin{bmatrix} i_d \\ i_q \end{bmatrix} + \begin{bmatrix} \frac{1}{L} & 0 & 0 \\ 0 & \frac{1}{L} & -\frac{\omega_r}{L} \end{bmatrix} \begin{bmatrix} u_d \\ u_q \\ \lambda_{mpm} \end{bmatrix} \tag{3.24}$$

$$C = \begin{bmatrix} 1 & 0 \\ 0 & 1 \end{bmatrix}$$

$$C = \begin{bmatrix} 1 & 0 \\ 0 & 1 \end{bmatrix}$$

The equation used to find the transfer function from u_d and $u_q$to i_d and i_q described in (3.25).

$$\begin{aligned} G(s) &= C(sI - A)^{-1} B \\ &= \begin{bmatrix} 1 & 0 \\ 0 & 1 \end{bmatrix} \left(\begin{bmatrix} s & 0 \\ 0 & s \end{bmatrix} - \begin{bmatrix} -\frac{R_s}{L} & \omega_r \\ -\omega_r & -\frac{R_s}{L} \end{bmatrix} \right)^{-1} \begin{bmatrix} \frac{1}{L} & 0 & 0 \\ 0 & \frac{1}{L} & -\frac{\omega_r}{L} \end{bmatrix} \\ &= \begin{bmatrix} g_{11}(s) & g_{12}(s) & g_{13}(s) \\ g_{21}(s) & g_{22}(s) & g_{23}(s) \end{bmatrix} \end{aligned} \tag{3.25}$$

The transfer functions can be expressed as:

$$g_{11} = \frac{s - \frac{R}{L}}{HL} \ ,$$

$$g_{12} = \frac{\omega_r}{HL} \ ,$$

$$g_{13} = \frac{\omega^2_r}{HL} \ ,$$

$$g_{21} = \frac{\omega_r}{HL} \ ,$$

$$g_{22} = \frac{s - \frac{R}{L}}{HL} \ ,$$

$$g_{23} = \frac{\left(s - \frac{R}{L}\right)\omega}{HL}$$

Where

$H = \ s^2 - 2s\frac{R}{L} + \frac{R^2}{L} + {\omega_r}^2$ Which is the determinant of matrix and used for the matrix inverse calculations. Six transfer functions are given by Equation (3.25). These transfer functions describe the liberalised system when the voltage equations are coupled due to λ_d and λ_q.

CHAPTER FOUR

CONTROLLER DESIGN FOR PMSM

4.1 Field oriented control (FOC) of PMSM

Field Oriented Control demonstrates how the orientation of the stator magnetomotive forces can control an induction motor or synchronous motor like a separately excited dc motor or current vector in relation to the rotor flux in order to achieve a desired goal it usually refers to controllers that keep an electrical angle of 90^o between the rotor and stator field components. The flux and torque producing currents in DC motors are orthogonal and can be controlled independently. These electromagnetomotive forces are also held to be orthogonal. The equation gives the torque developed.

$$T_e = K_a \emptyset(I_f) I_a \tag{4.1}$$

As a result, the flux is solely determined by the field winding current. If the flux remains constant, the armature current can be used to control the torque. As a result, DC machines are said to have decoupled or independent torque and flux control. The stator and rotor fields are not orthogonal in AC machines. The stator current is the only one that can be controlled. Field Oriented Control is a technique for decoupling torque and flux by transforming stator current quantities (phase currents) from a stationary reference frame to torque and flux producing current components in a rotating reference frame.

FOC has the following advantages:

- Transformation of a complex and coupled AC model into a simple linear system
- Independent control of torque and flux, similar to a DC motor
- Fast dynamic response and good transient and steady state performance
- High torque and low current at start up
- High Efficiency

Because of the benefits mentioned above, FOC-based techniques of PMSM speed control were considered in this thesis. The FOC technique entails converting the stationary three reference frames into rotating two reference frames in which the following tasks are carried out. According to Author [21] the FOC technique entails converting the stationary three reference frames into rotating two reference frames in which the following tasks are carried out.

1. Stator reference frame (a, b, c) in which a, b, c are coplanar, at 120 degrees to each other.
2. An orthogonal reference frame (α, β) in the same plane as the stator reference frame, with a 90-degree angle between the two axes instead of a 120-degree angle. In the second frame, the alpha-axis is parallel to the a-axis.
3. The d-axis is perpendicular to the d-axis and parallel to either the rotor's flux vector or the N and S poles in the rotor reference frame (d, q).

4.1.1 Control Design

The controller's primary function is to regulate the machine's speed. To accomplish this, a cascade control structure is used, with the outer loop acting as a speed controller and the inner loop containing two current controllers. The d-axis current and q-axis currents are controlled by two current controllers. The speed controller calculates the reference q-axis current based on the determined necessary torque to maintain the speed reference. To avoid interference between the controllers, the bandwidth of the outer loop should be $5 \sim 10$ times lower than that of the inner loop in this control structure. The control loops are designed as a continuous transfer function, and then discretized transfer functions with similar properties are discovered. This is accomplished by taking into account the system's delays as well as the sampling frequency.

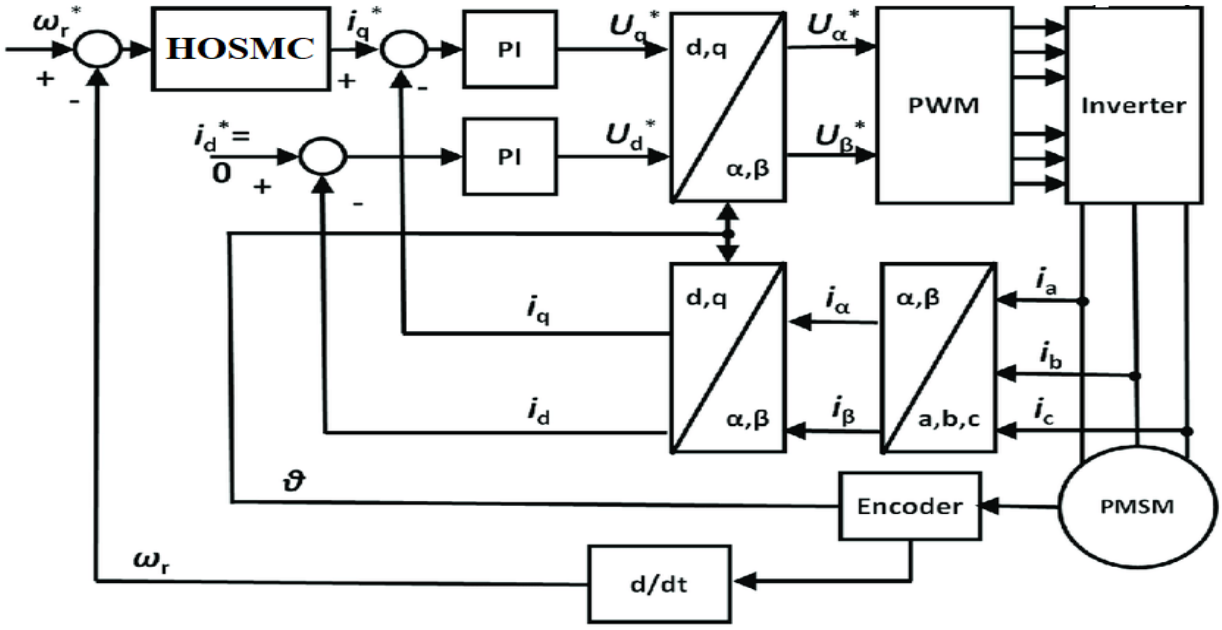

Figure 4.1 Field Oriented Control based speed control of PMSM using HOSM controller

4.1.2 Design of Current Controllers

The inner loop that controls the stator currents is controlled by the current controllers. From the design specification the damping coefficient (ζ) and undammed natural frequency (ω_n) are assigned as in equation (4.2 and 4.3)

$$\zeta \geq 0.48, \omega_n \geq 1500 rad/sec \tag{4.2}$$

Using the equation, the damping coefficient and natural frequency are chosen to be:

$$\zeta = 0.7, \omega_n = 1500 rad/sec \tag{4.3}$$

From the figure 4.2 and 4.3 the overall second order transfer function T(s) obtained between the torque component i_q and its reference i_q^* is given as:

$$T(s) = \frac{i_q}{i_q^*} = \frac{k_p x s + k_i}{L_q s^2 + (R_s + K_p)s + K_i} \tag{4.4}$$

The equation of second order closed loop system is given as:

$$T(s) = \frac{\omega_n^2}{s^2 + 2\zeta\omega_n s + \omega_n^2} \tag{4.5}$$

The values of Kp and Ki are determined by comparing the denominator of eqn 4.4 and eqn 4.5 for inner loop (current loop).

Based on motor simulation parameter given in appendix

$$K_p = 2\zeta\omega_n L_q - R_s$$

$$K_i = \omega_n^2 x L_q$$

In this thesis, damping ratio (ζ) and natural frequency (ωn) to be selected as 0.7 and 1500 red/sec respectively.

The transfer functions for the system are derived using the voltage equations for both the q-axis and the d-axis. When the voltage equations found in equation (3.15) are transformed to the Laplace domain, the following results are obtained:

$$i_d = \frac{v_d + \omega_r L_q i_q - s\lambda_{mpm}}{sL_d + R_s} \tag{4.6}$$

Where $s\lambda_{mpm} = 0$

$$i_q = \frac{v_q - \omega_r\left(L_d i_d + \lambda_{mpm}\right)}{sL_q + R_s} \tag{4.7}$$

The system is now coupled, as seen in the motor voltage equations (4.6), and (4.7). However, the system can be decoupled by compensating for the back EMF disturbance.

After decoupling the system, the transfer function for both the q-and d-axes is calculated, as shown in equations (4.8) and (4.9).

$$G_d = \frac{i_d}{v_d} = \frac{1}{sL_d + R_s} \tag{4.8}$$

$$G_q = \frac{i_q}{v_q} = \frac{1}{sL_q + R_s} \tag{4.9}$$

Figures 4.2 and 4.3 depict the complete control loop for d- and q-axis current.

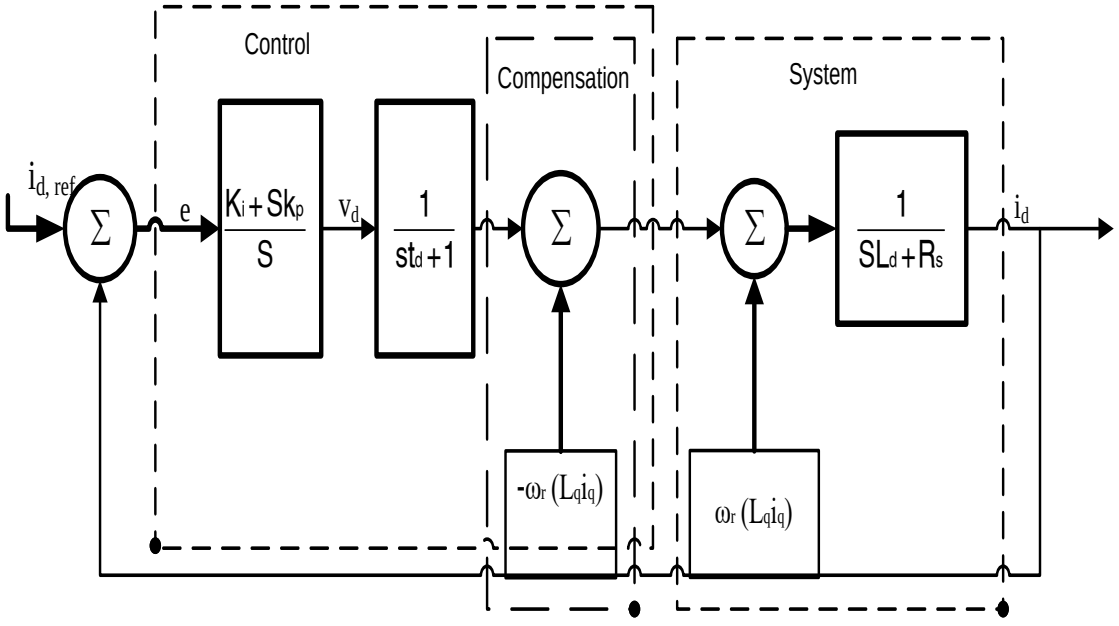

Figure 4.2 Control loop for d-axis current

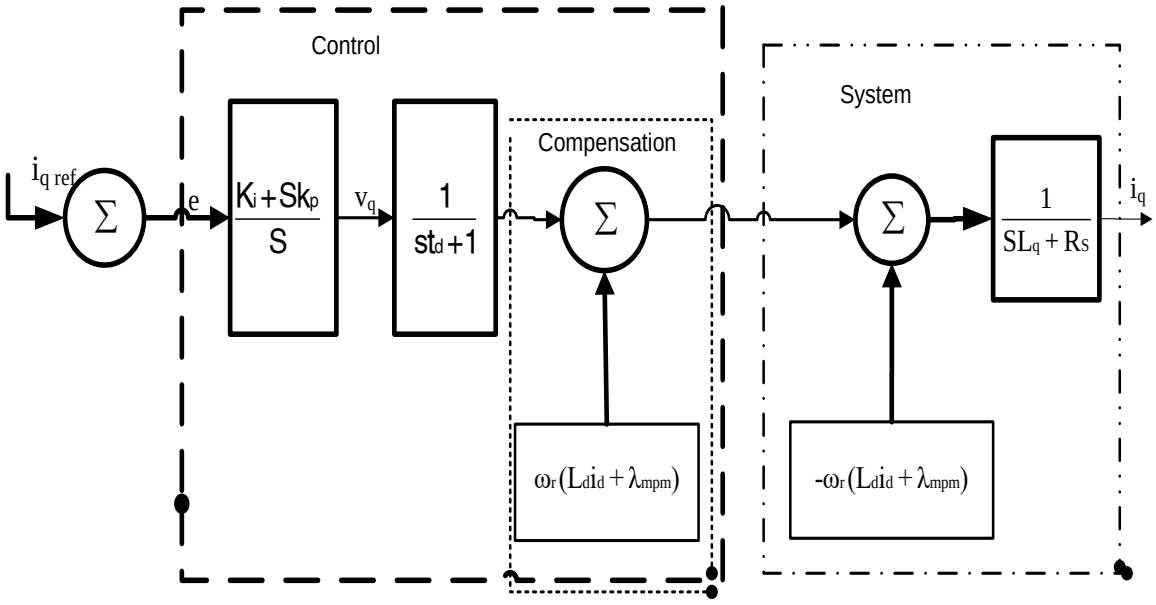

Figure 4.3 Control loop for q-axis current

Equation (4.10) depicts the resulting open-loop transfer function, which includes the controller and delays. v_d

$$G_{ol}(s) = \frac{K_i + sK_p}{s} \frac{1}{st_d + 1} \frac{1}{sL_d + R_s} \tag{4.10}$$

The total time delay will be

$$f_s = 5kHz \tag{4.11}$$

$$t_s = \frac{1}{f_s}$$

$$t_d = 1.5t_s$$

Where the sampling frequency of the system is atfs. A first-order system, which is effectively a low pass filter, can approximate the delay. The transfer function is shown in equation (4.12).

$$G_d = \frac{1}{st_d + 1} \tag{4.12}$$

4.1.3 Design of Speed Controllers

The goal is to create an appropriate control that ensures robust performance in the presence of parameter and load variations. A PI controller is also a good choice here because it can effectively compensate for the system's torque disturbances. The controller also improves the system's transient response. The speed loop is expected to be much slower than the current

loops. As a result, a first-order system with the same settling time as the actual current loops will approximate the current loops.

The inner loop is modified to the first order system from the third order. Now the time constant is derived by $= \frac{t_{settling}}{4}$. Then transfer function becomes:

$$G_{IL} = \frac{1}{\tau s + 1} \tag{4.13}$$

The transfer function for the mechanical system

$$T_e = J\frac{d\omega_m}{dt} + B_m\omega_m + T_{dist} \tag{4.14}$$

Equation (4.14) is transformed into the Laplace domain with the disturbances set to zero to ensure that controllers are designed with the highest overshoot. The mechanical system's transfer function is formed by combining (3.21) and (4.14), yielding the following equation:[24]

$$\frac{\omega_m}{i_q} = \frac{K_{C2T}}{Js + B_m} \tag{4.15}$$

Where $K_{C2T} = \frac{3}{2}N_{pp}\lambda_{mpm}$

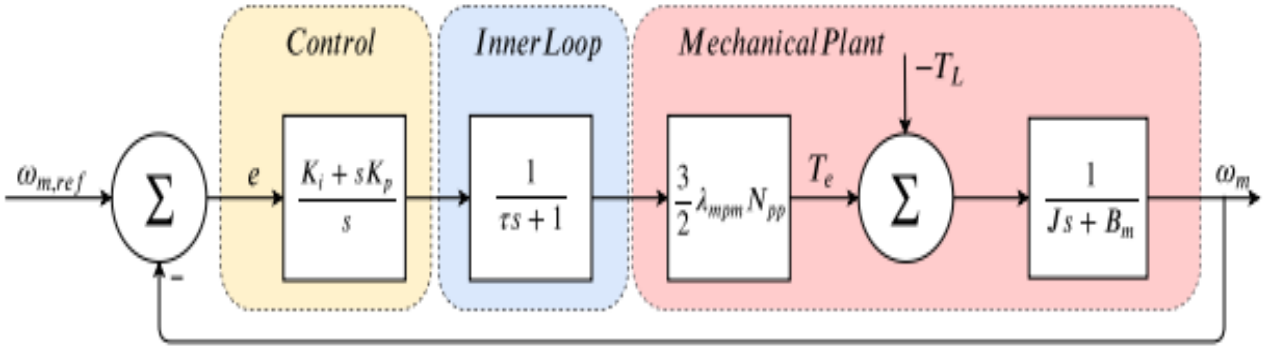

Figure 4.4 Block diagram of the speed loop.

4.2 High Order Sliding Mode Control For PMSM

Due to their inherent benefits, permanent magnet synchronous motors are perfect for contemporary applications for industrial control. On the other hand, synchronous motor the A typical example of a nonlinear, multivariable, coupled system. As a result, several methods, including accurate feedback linearization control, have been developed in recent years to enhance the performance of motor control. However, It is impossible to have a complete understanding of all synchronous motors. properties in a dynamic system. The environment

will affect the system parameters in the equation, such as resistors and inductors, which will alter when the ambient temperature varies. To provide powerful dynamic performance in the presence of parameter uncertainty and outside disturbances, a robust controller must be designed. Based on this idea, a sliding mode control has been devised and put into practice. The sliding mode controller is the fundamental component of switching feedback control at high frequencies. Depending on the system stateits governing laws switching value varies. The sliding surface and the control rule are the two components of the sliding mode controller. The dynamic system is hence constrained around the sliding mode surface.This is also referred to as a sliding mode state, which solely applies to the selected sliding surface. It is impossible for outside factors to affect the sliding state dynamic system. Maintaining a carefully selected constraint in sliding mode at zero is the basic goal of sliding mode control. A logical way to categorize the degree of smoothness of the constraint function derived along the system trajectories determines the sliding modes. [21]. last few years have seen the widespread deployment of a novel high order sliding mode control. The original discrete control has been replaced with a high order derivative of the variables in sliding mode, which prevents chattering when producing high order differentiating.

A switch role in conventional control for the sliding mode typically depends as to the state of the system and is unrelated to the control input. Items that are discontinuous will be sent straight to the controller. On the other hand, the high order sliding mode control moves the utilizing the differentiations of the sliding mode control variable create a new sliding mode surface by adding discrete basics to the sliding mode variable's first or higher order derivative. [4]. High order sliding mode control does not just stop chattering issues from occurring. affect standard sliding mode control, but also gets around the restriction that the relative degree in the control law design must be equal to 1. The technology permits discontinuous item variables to be sent to the first order or high derivative of the order of the sliding mode in order to avoid chattering while still maintaining the strong resilience of the classic sliding mode control. The controller's architecture also eliminates the requirement for a relative degree of 1. As a result, developing the sliding mode surface's parameters is significantly streamlined. The Nesting sliding mode controllers and quasi-continuous sliding mode controllers are the two most well-known r-sliding mode controller families. [25]

$$u = -\alpha \psi_{r-1,r}(\sigma, \dot{\sigma}, ..., \sigma^{(r-1)}) \tag{4.16}$$

This is defined recursive procedures have magnitude $\sigma > 0$, and solve the general output regulation problem for system ($\sigma^{(r)} \in [-C, C] + [K_m, K_M]u$). The parameters of the controllers can be chosen in advance for each relative degree r. r. Only the magnitude α must be adjusted for any fixed C, K_m, K_M , most conveniently by computer simulation, thus avoiding complex and excessively large estimates.

Controllers for Quasi-continuous Sliding Mode

The controlled in nested sliding mode display high frequency leaps When they get closer to the HOSM, of transient trajectories. Even though the magnitude of the leap tends to be zero. throughout the transitory, it can still be problematic in real-world applications.

Think about the nonlinear system below, which has a smooth output function. [25][4]

$$\begin{aligned} \dot{X} &= f(t,x) + g(t,x)u \\ y &= \sigma(t,x) \end{aligned} \tag{4.17}$$

where $X \in R^n$ g and f , $\sigma : R^{n+1} \to R$ are unidentified smooth operations, $u \in \square$, Moreover, n confusing. presenting a new coordinate variation $\xi_1 = \sigma, \xi_2 = \sigma_2, ...\xi_r = \sigma^{(r-1)}$ where r is the relative degree of the system which is assumed to be constant and known, i.e

$$\sigma^{(r)} = F(t,x) + G(t,x)u \tag{4.18}$$

Where $F(t,x) = \sigma^{(r)}\big|_{u=0}, G(t,x) = \left.\frac{\partial \sigma^r}{\partial u}\right|_{u \neq 0}$, it is supposed that for some $K_m, K_M, C > 0$ the following inequalities hold at least locally $0 < K_m \leq \frac{\partial \sigma^r}{\partial u} \leq K_M, \sigma^r\big|_{u=0} \leq C$.

At the very least, the HOSM should have a discontinuous control rule in Equation (4.16). [25]

$$\sigma = \dot{\sigma} = ... = \sigma^{(r-1)} = 0 \tag{4.19}$$

If an r-sliding controller of equation (4.16) is continuous everywhere except at equation, it is said to be quasi-continuous (4.19)

The following examples demonstrate how the system is finitely stabilized at the origin.

Theorem: Assuming that the $\beta_1, \beta_2, \beta_3, ...\beta_{r-1}, \alpha > 0$ are chosen in the lexicographic sequence to be suitably large, the controller Eqn. (4.12) is a homogeneous r-sliding controller that guarantees stability in finite time, (4.17) [25][4].

$$\begin{gathered} \varphi_{0,r} = \sigma, N_{0,r} = |\sigma|, \psi_{0,r} = \frac{\varphi_{0.r}}{N_{0,r}} = sign(\sigma) \\ \varphi_{i,r} = \sigma^{(i)} + \beta_i N_{(i-1),r}^{(r-i)/(r-i+1)} \psi_{i-1,r} \\ N_{i,r} = \sigma^{(i)} + \beta_i N_{(i-1),r}^{(r-i)/(r-i+1)} \psi_{i-1,r} \\ \psi_{i,r} = \varphi_{i,r/N_{i,r}} \end{gathered} \tag{4.20}$$

Furthermore $N_{i,r}$ is positive definite, ($N_{i.r} = 0, \sigma = \dot{\sigma} = ... = \sigma^{(r-1)} = 0.$ the inequality $\left|\psi_{r-1,r}(\sigma, \dot{\sigma}, ..., \sigma^{(r-1)})\right|$ holds whenever $N_{i,r} > 0$ for $i = 1, ...r-1$.

The function $\psi_{r-1,r}(\sigma, \dot{\sigma}, ...\sigma^{(r-1)})$ is constant all over the place but the detail $\sigma = \dot{\sigma} = ... = \sigma^{(r-1)} = 0$. The choice of parameters $\beta_1, \beta_2 .... \beta_{r-1}, \alpha > 0$ selects a controller type that can be used by altogether schemes. (3.21) of comparative step r. The parameter is select exactly for at all fixed K_m, K_M, C, computer imitation, conveniently evading repetitively high estimates of K_m, K_M, C.

The following are quasi-continuous controllers of eqn. (4.16) with , which have simulation tested: [25]

$$\begin{gathered} r = 1: u = -\alpha sign(\sigma) \\ r = 2: u = -\alpha \frac{\dot{\sigma} + |\sigma|^{1/2} sign(\sigma)}{|\dot{\sigma}| + |\sigma|^{1/2}} \\ r = 3: u = -\alpha \frac{\ddot{\sigma} + 2(|\dot{\sigma}| + |\sigma|^{2/3})^{-1/2}(\dot{\sigma} + |\sigma| sign(\sigma}{|\ddot{\sigma}| + 2(|\dot{\sigma}| + |\sigma|^{2/3})^{1/2}} \end{gathered} \tag{4.21}$$

4.3 Estimator Design

The dq-reference frame transformation, which linearizes the system, is the foundation of FOC. This allows for the use of simple PI controllers to control both the current and the speed. A precise position signal is required for the reference frame transformation. As a result, the position is the most important state to estimate. A large position error will also result in reduced torque output and as a result, reduced motor power. Because the full iq current from the VSI

is not available, some of it will be id current. Figure 4.5 illustrates this. The cosine of the position error angle determines the load torque loss. This also implies that the motor's operation would be less efficient than it could be. This must be avoided to the greatest extent possible.

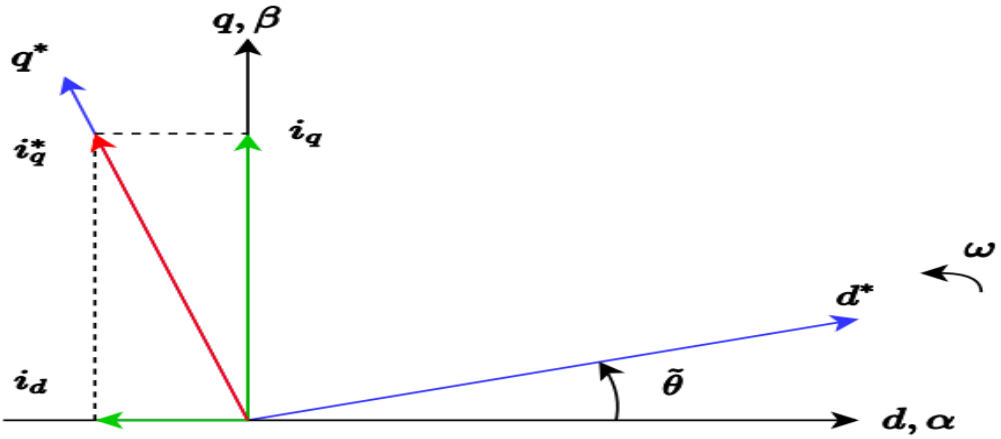

Figure 4.5 The influence of angle error ($\tilde{\theta}$) on actual stator iq current [8]

It is necessary to convert the stator voltage equations from the dq-reference frame to the $\alpha\beta$ - reference frame. The rotating speed of the reference in the $\alpha\beta$ -reference frame is zero because the reference-frame is now stationary. This is advantageous because both the position (θ) and the speed (ω r) will appear in the back-EMF equations. The new voltage equations in vector form are shown in equations (4.18).

$$\begin{aligned} \vec{v}_{\alpha\beta} &= R\vec{i}_{\alpha\beta} + p\vec{\lambda}_{\alpha\beta} \\ \lambda_{\alpha\beta} &= (L_d i_d + \lambda_{mpm} + jL_q i_q)e^{j\theta_r} \end{aligned} \tag{4.22}$$

As previously stated, the position appears in the back-EMF components, as illustrated in equation (4.19)

$$\begin{aligned} e_\alpha &= -\lambda_{mpm}\omega_{r,el}\sin\theta_r \\ e_\beta &= \lambda_{mpm\omega_{r,el}}\cos\theta_r \end{aligned} \tag{4.23}$$

Equation (4.23) can be used to calculate θ_r from the, α – components of the back-EMF (4.24). Figure 4.6 depicts this as well.

$$\hat{\theta} = \tan^{-1}\left(\frac{-\hat{e}_\alpha}{\hat{e}_\beta}\right) \tag{4.24}$$

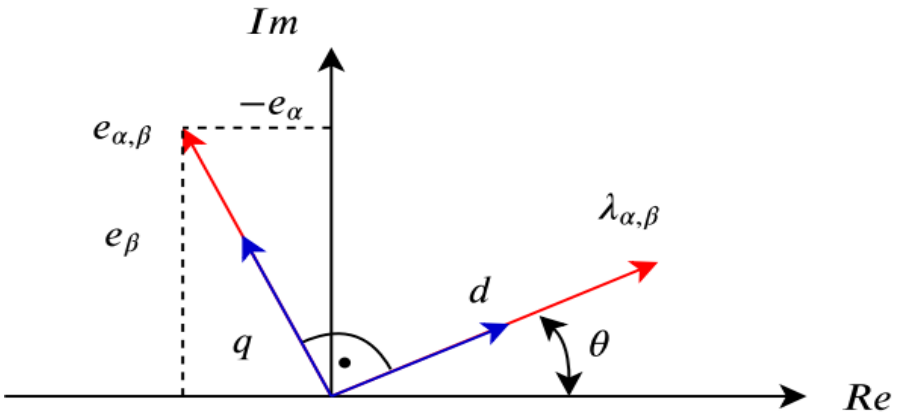

Figure 4.6 The relation between $\boldsymbol{e_{\alpha\beta}}$ and $\boldsymbol{\lambda_{\alpha\beta}}$ and vectors and the rotor position $\boldsymbol{\theta}$ [8]

The position can also be calculated from estimated flux-linkage because, assuming that the stator resistance is neglectable, the relationship between flux-linkage and back-EMF voltage is as follows:

$$\vec{\lambda}_{\alpha\beta} = \int \vec{v}_{\alpha\beta} dt \tag{4.25}$$

Integration or differentiation can be represented graphically a 90° rotation between the vectors. The direction of rotation is what distinguishes integration from differentiation. Combining the equations in (4.23), a dense formula (4.26) for rotor speed (ω_r) estimation can be obtained, but care must be taken when using the equation. It is extremely sensitive to the λ_{mpm} parameter, which serves as a scaling factor in this case. If an accurate λ_{mpm} can be obtained by measuring it online or offline, this formula can provide a better speed signal than methods that use specific mathematical tools to differentiate the position.

$$|\omega_r| = \frac{1}{\lambda_{mpm}} \sqrt{e_\alpha^2 + e_\beta^2} \tag{4.26}$$

In other cases, where λ_{mpm} is uncertain, obtaining the speed is easier by differentiating the position and filtering the signal, as shown in figure 4.7, or by using a Phase-locked loop structure, as shown in figure 4.8.

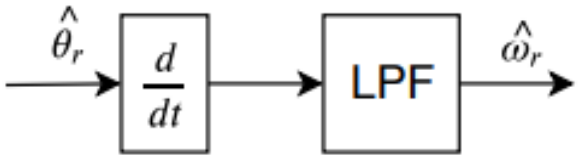

Figure 4.7 Structure of differentiating a signal

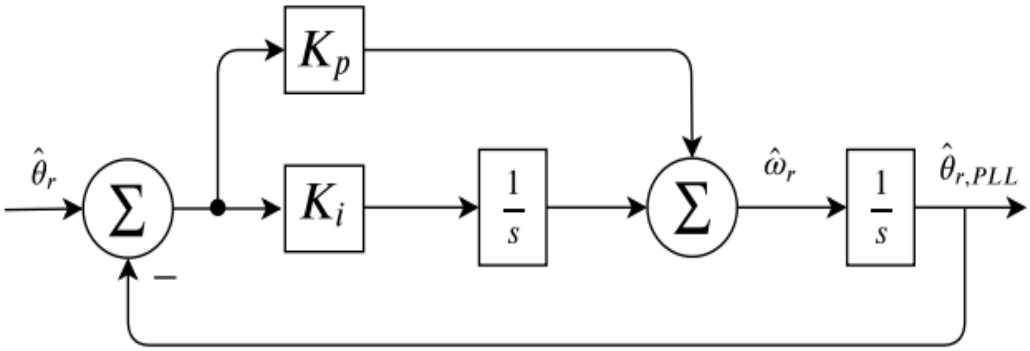

Figure 4.8 The phase-locked loop

The PLL structure was thoroughly examined in [14]. The error signal is written as follows:

$$\tilde{\theta} = \hat{\theta}_r - \hat{\theta}_{r,PLL} \tag{4.27}$$

The open-loop transfer function is then presented in equation form (4.28)

$$\hat{\theta}_{r,PLL} = \tilde{\theta}_r(K_p + K_i\frac{1}{s})\frac{1}{s} \tag{4.28}$$

When the loop is closed, the expression shown in equation is obtained (4.29).

$$H_{PLL,\theta}(s) = \frac{\hat{\theta}_{r,PLL}}{\hat{\theta}_r} = \frac{K_p s + K_i}{S + K_p s + K_i} \tag{4.29}$$

4.4 Space Vector Pulse Width Modulation

The VSI has voltage error at low speeds due to non-linear effects. Dead time, on/off switching device delays and voltage drops in the inverter all contribute to VSI non-linearities [26]. Because the estimator uses the voltage signal (among other signals) for calculations, these effects distort the voltage, resulting in an error in the estimated signals. The voltage is not directly measured, but rather assumed to be the commanded voltage, which is the source of some of the estimation errors. Directly measuring stator voltages is difficult because the voltage is made up of pulses. Filtering the voltage would then be required, but filtering introduces phase lag into the system, which is unacceptable [27]. As a result, a compensation method is required to reduce the average voltage error to zero.

4.4.1 Analysis of the VSI voltage error

A voltage source inverter (VSI) is a power converter that generates an alternating current (AC) output waveform from a direct current (DC) voltage source input. The VSI can control the alternating current output voltage. To emulate a three-phase sinusoidal waveform, the inverter

controls the magnitude and frequency of the output using a modulation technique such as Space vector modulation.

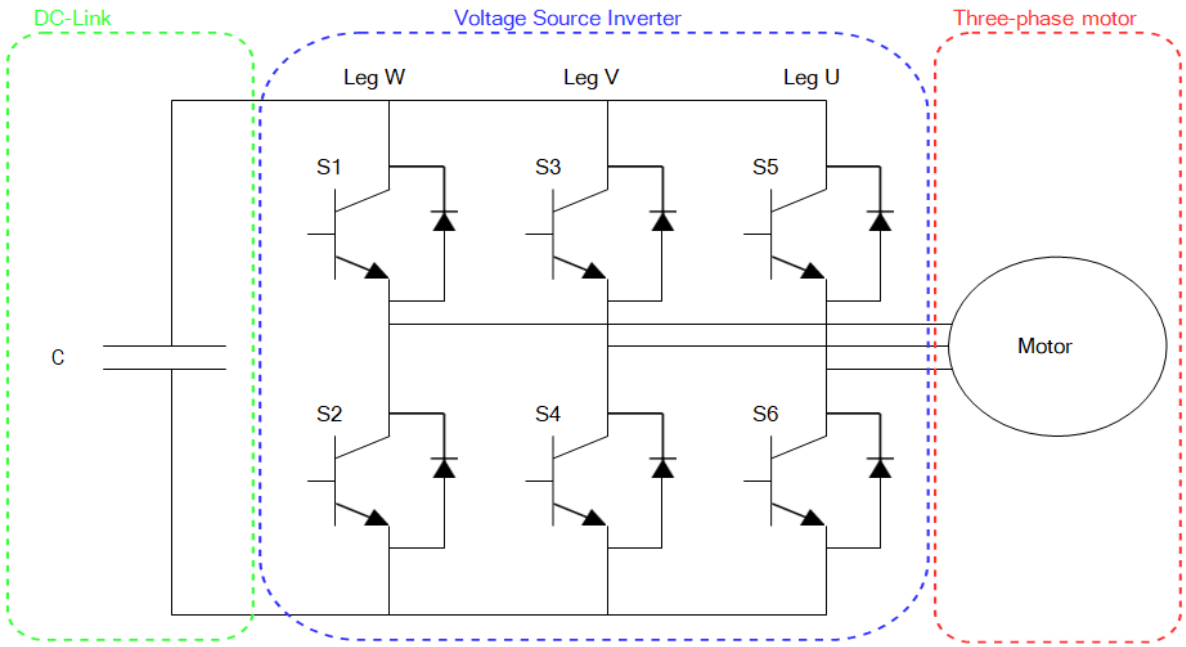

Figure 4.9 Three Phase inverter

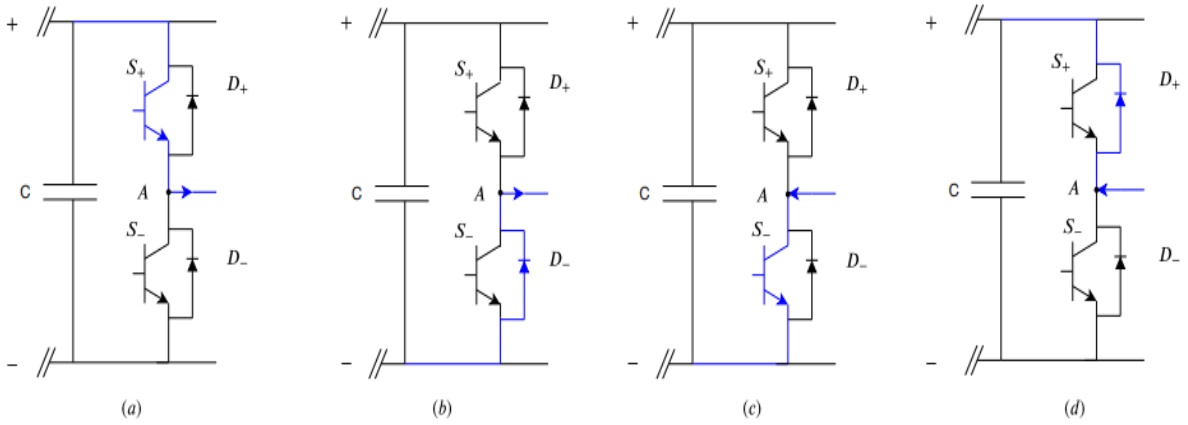

Figure 4.10 The four possible states of one leg when the dead time effect

If only the switch is conducting (figures (a), (c)), the gate signal can turn the switch off, which immediately stops the current flowing in that direction. There is no dead time effect as a result of this. The dead time effect occurs when the diode is conducting (figures (b), (d)), because the diode cannot be closed immediately. This is because the system contains an inductive load (the motor). The dead time effect occurs between the dotted lines, as shown in figure 4.11. For the time being, only the case where the current is positive i > 0) will be considered. The upper

switch is open, and the voltage at point A equals Vdc -Von. The switch (S+) is then turned off. Both switches are now open and current flows through the lower diode. Point A's voltage is the same as the voltage drop on the diode right now. When the switch (S-) is turned on, the lower diode continues to conduct and the forward voltage remains constant because the diode and the switch are in parallel. As a next step, (S-) is disabled. Even after that, the current continues to flow because the diode continues to conduct until the switch (S+) is turned back on after the specified dead time. The voltage at point A is now equal to its initial value. This case study results in a decrease in the average voltage in the system. If the current direction is negative (i <0), the upper switch (S+) open first and the parallel diode conducts. As aresult, the voltage at point A is Vdc + VD. When (S+) is turned off, (D+) continues to conduct until the other switch is activated.

It is similar to how it was previously explained. This case study results in a positive gain in the system's average voltage.

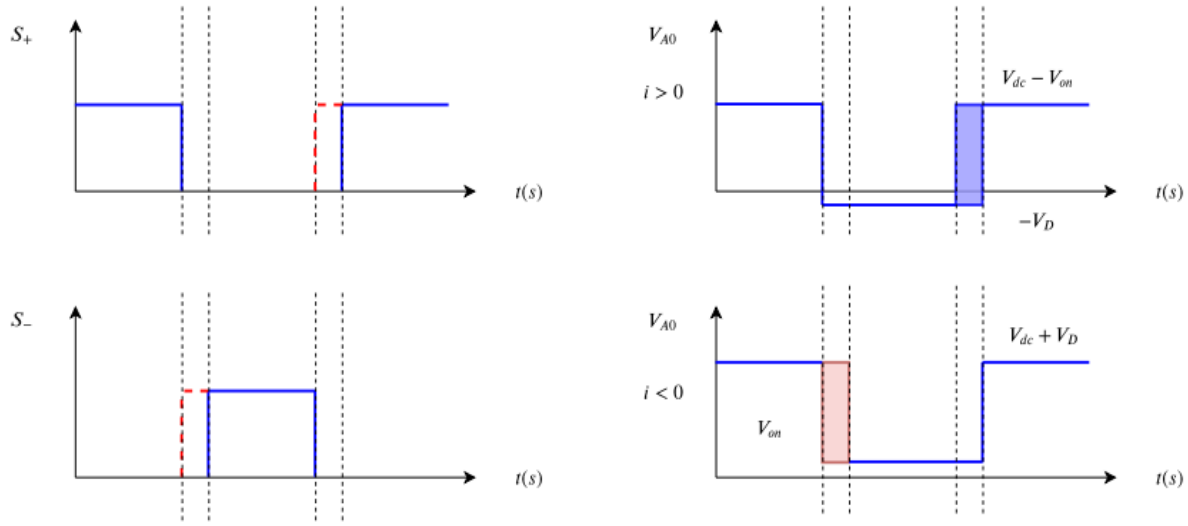

Figure 4.11 The dead time effect for one sequence when the current is positive.

Where V_{dc} is the power supply voltage, V_{on} is the voltage drop across the swith the voltage drop across the swith, and VD is the voltage drop across the diode [28]. Further investigation reveals that the voltage cannot be changed immediately due to the snubber capacitor in the system. The snubber capacitor is connected in series with the diode and switching device. As a result, the dead time effect is nonlinear and can be represented by the equation [29]:

$$\Delta v = \frac{i}{C_{snubber}} \Delta t \tag{4.30}$$

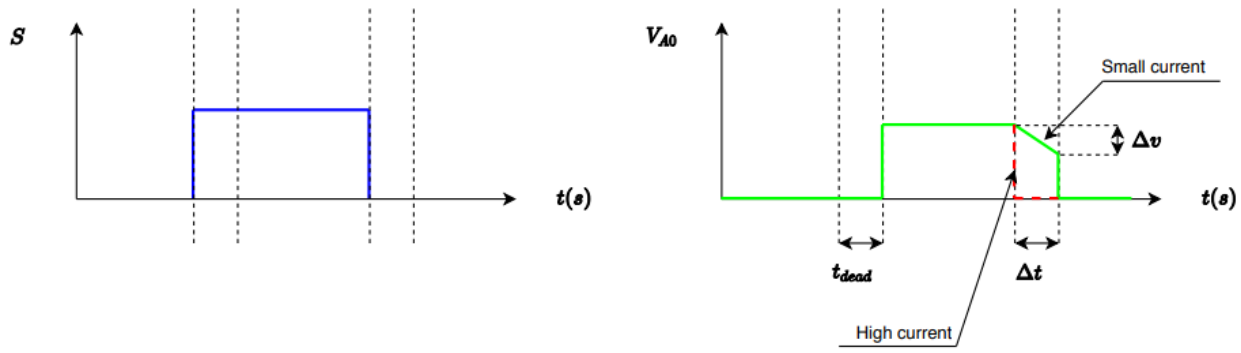

Figure 4.12 The effect of the snubber capacitor on the dead time effect.

4.4.2 Modulation Technique

Modulation is accomplished by properly selecting an inverter switching state for each sampling period and then calculating the appropriate time for each state. According to the simplefied schematic of the VSI above, figure, there are six switches that can be turned on or off. However, the switches are in pairs, with S1 and S2 forming one leg, so the total number of the switching states is $2^3 = 8$. Six of the eight vector configurations correspond to different applied voltages. The other two are zero vectors, which occur when there is no voltage on the terminals. These vectors are split into six sectors, each representing a different pair of switches. Figure 4.13 shows how a binary number can be formed for each vector by representing each leg of the inverter with 1 for on state (top switch closed and bottom switch open) and 0 for off state (top switch open and bottom switch closed) [30].

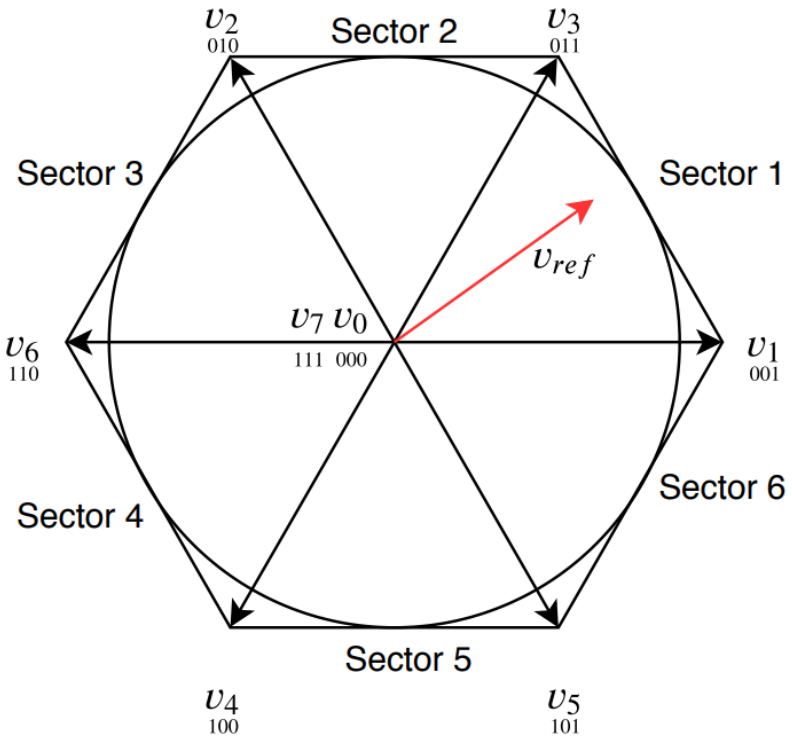

Figure 4.13 Vectors and zero vectors inside the stator [21]

These vectors are split into six sectors, each representing a different pair of switches. Figure 4.13 shows how a binary number can be formed for each vector by representing each leg of the inverter with 1 for on state (top switch closed and bottom switch open) and 0 for off state (top switch open and bottom switch closed).

A space vector serves as the reference. This vector is obtained by combining the balanced abc voltage vectors. This indicates that the space vector is located in the $\alpha\beta$ -reference frame. The following equations are used to calculate the amplitude and angle of the and angle space vector.

$$V_{ref} = \sqrt{v_\alpha^2 + v_\beta^2}$$
$$\theta = \tan^{-1}(\frac{v_\beta}{\alpha}) \quad (4.31)$$

The reference voltage vector's location and the vector that will be used to include it are determined by equation (4.32). [7]

$$\theta_k = \theta - (k-1)\frac{\pi}{3} \quad \text{for } 0 \le \theta_k \le \frac{\pi}{3} \quad (4.32)$$

Where k is the sector number

The desired reference voltage is then converted to on/off binary signals for each leg of the inverter, which are referred to as duty cycles. The duty cycles $d_x, d_y, and\ d_z$ represent the active vectors and the zero vectors, respectively. The zero vectors are made equal in space vector modulation. By distorting the wave around the peak values, the modulated sinusoidal wave differs from the ideal one. The duty cycles givens as eqn. (4.33), with sector 1 from Figure 4.14 as an example.

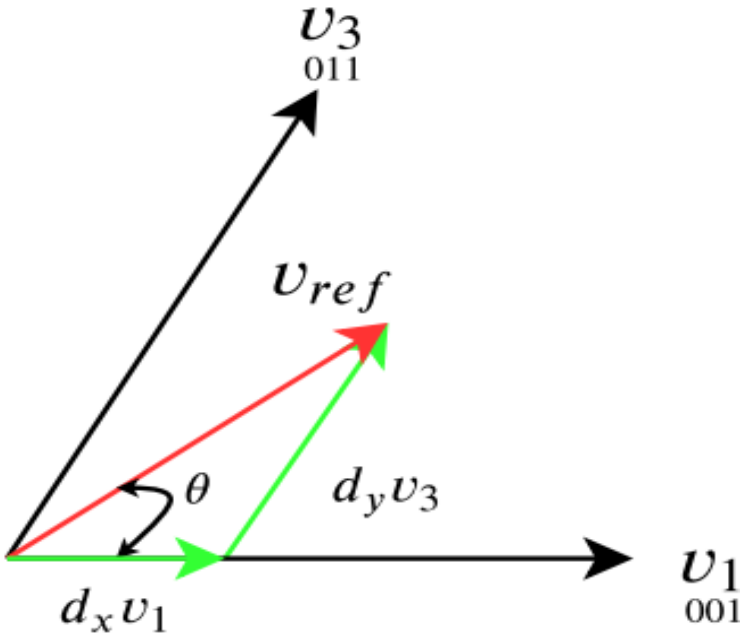

Figure 4.14 Sector 1 with reference vector [8]

$$\vec{v}_{ref} = d_x \vec{v}_1 + d_y \vec{v}_3 \tag{4.33}$$

For the other sectors the equation can be retten as

$$\begin{aligned} d_x &= \frac{\sqrt{3v_{ref}}}{v_1}\frac{2}{3}\sin\left(\frac{\pi}{3}-\theta\right) \\ d_y &= \frac{\sqrt{3v_{ref}}}{v_3}\frac{2}{3}\sin(\theta) \\ d_z &= t-(d_x+d_y) \end{aligned} \tag{4.34}$$

Where v_{ref} and are known, t represents the sampling period [27]

The same procedure can be used for sectors 2–6 if 'k' is used instead of for the kth sector. Finally, the appropriate gate signals are generated using the space vector sequence. To reduce the switching frequency, the switching sequence must be configured so that the transition from

one section to the next section is accomplished by switching only one leg at a time. Because the zero vectors are the same, the time interval dz is divided and distributed equally at the start and end of the sampling period ‘t’. Each period's duty cycle adds up to the sampling period ‘t’. The switching sequence for the reference vector in sector 1 is V0, V1, V3, V7, V3, V1, and V0. Each inverter switch is only turned on and off once per sampling period.

CHAPTER FIVE

SIMULATION RESULTS AND DISCUSSION

5.1 Introduction

Currently, the speed controller in the PMSM speed regulation vector control system uses traditional regulation. However, as previously stated, PMSM is a nonlinear, strongly coupled multivariable system when the control system is affected by external or electrical disturbances. When the machine's internal parameters change the traditional control method cannot meet the actual requirements. As a result, high order sliding mode is used to improve the dynamic quality of the PMSM speed control system (HOSMC).The design of high order sliding mode speed controller will be introduced in this section due to its advantages of insensitivity to motion and parameters and fast response speed. As shown in figure 4.1 MatLab/Simulink R2018a was used to construct the simulator for controlling the PMSM's speed using the HOSM controller. The simulation conditions are set as: DC side voltage $U_{dc} = 3\,11V$, PWM frequency is set to $f_{PWM} = 10\ kHz$, the period is set to $T_s = 10\mu s$ and the relative tolerance is set to 0.0001 and the simulation time is set to 0.4s.

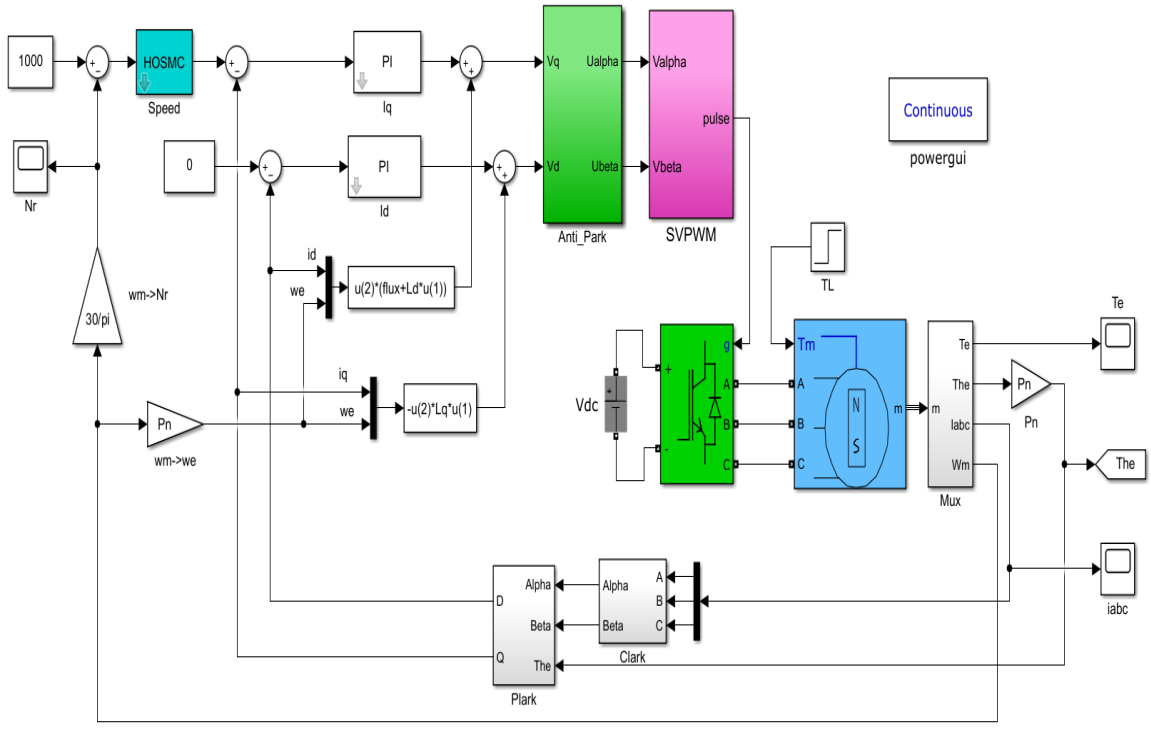

Figure 5.1 PMSM vector control simulation model based on HOSM speed controller

The simulation block diagram of a Space Vector Pulse Width Modulated signal is shown in Figure 5.2. SVPWM block is a Matlab source code embedded on simulation block that takes state voltage in alpha and beta directions as input and outputs six PWM generated pulses. To generate a pulse width modulated signal, the output operation times $T_{cm1}, T_{cm2},$ and T_{cm3} are compared to a saw tooth repeating sequence signal with the same frequency as PWM. Finally, the three output signals are fed into an inverter logic operator, which generates the inverse of them. A three-phase voltage source inverter is driven by these six pulse width modulated signals.

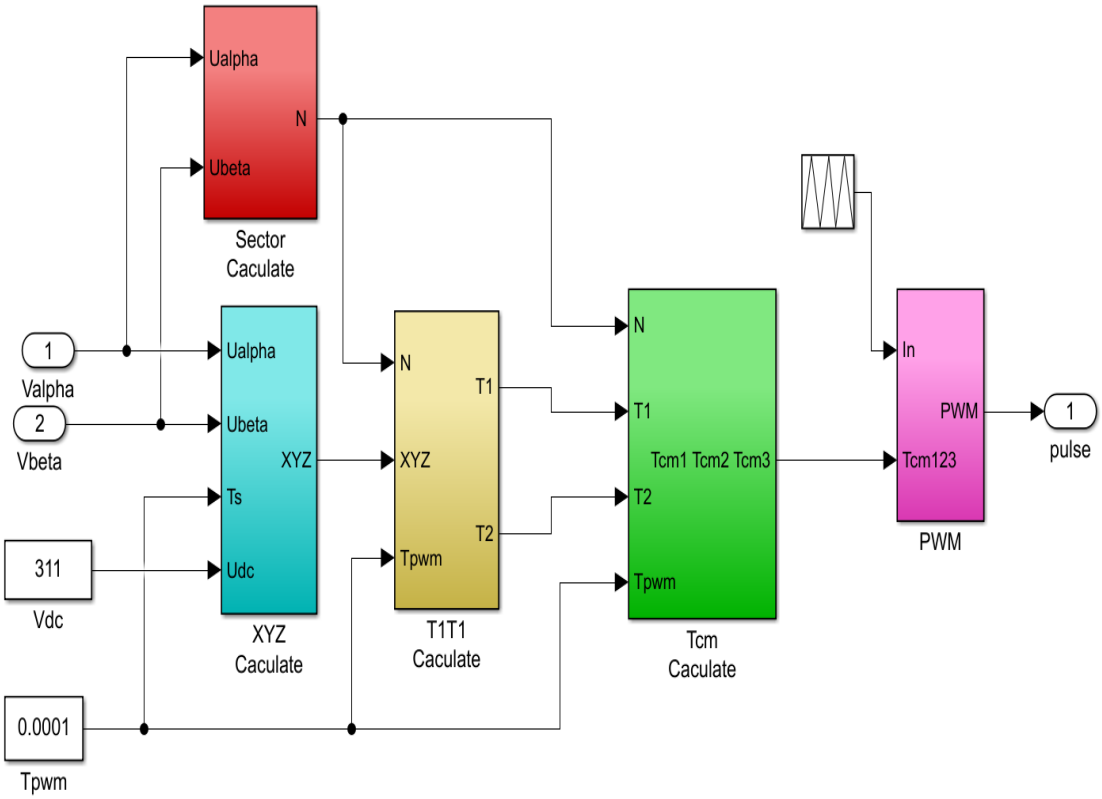

Figure 5.2 Diagram for the SVPWM generating simulation

5.2 Simulation Modeling and Result Analysis

The PMSM's Over all Mat Lab/Simulink model allows simulation of the machine's behavior and high order sliding mode controller for different operating modes. As a result, the Results from simulations were utilized to assess its performance. Table A1.1 of Appendix A contains the PMSM parameters used in the simulation. The goal of High order sliding mode control chattering is eliminated by acting on high order sliding mode surfaces. Figure 5.3 illustrate the

motor's speed response When Commonded with a reference speed of 104.7 rad/sec (1000RPM).

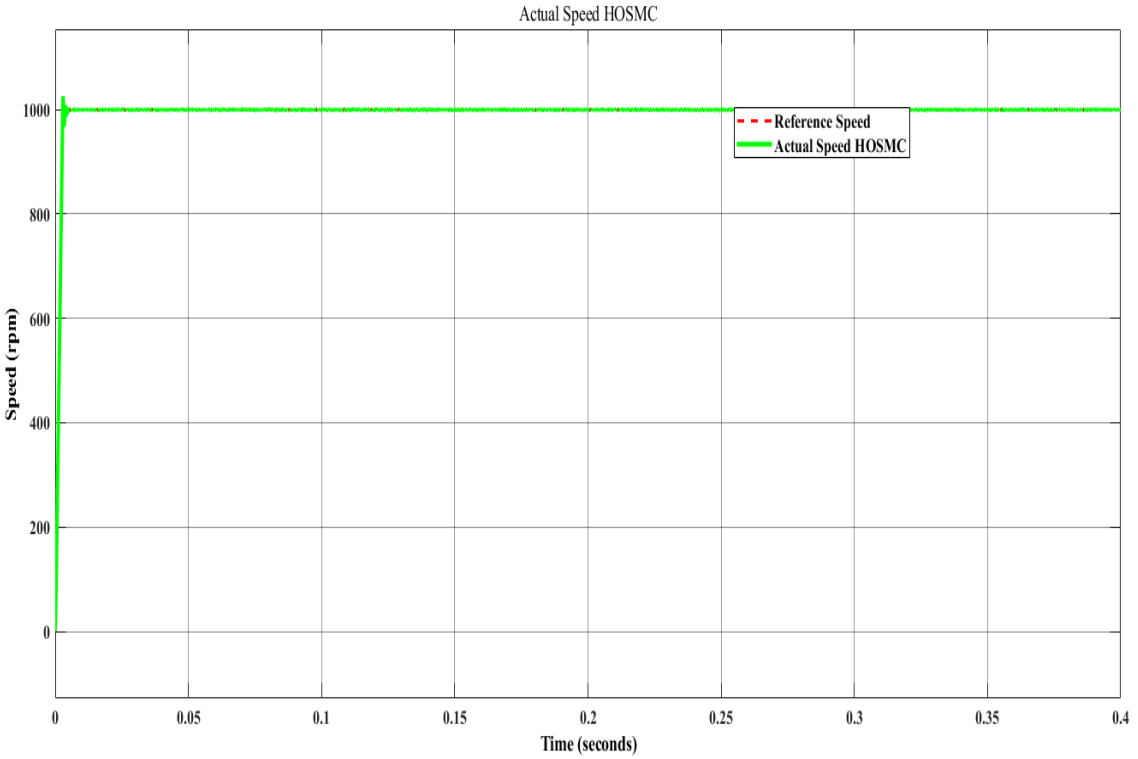

Figure 5.3 The PMSM's response Speed under no load conditions.

The above figure 5.3 shows a variation in speed of a motor over time. The stable rate of change The steady state speed corresponds to the Commonded at a reference speed With a rising time of 2.152 mili seconds the system is able to adapt to the reference signal.miliseconds, 2.065 seconds for settling and a maximum overshoot value of 2.577%, indicating that it has a high steady-state and transient responsiveness.

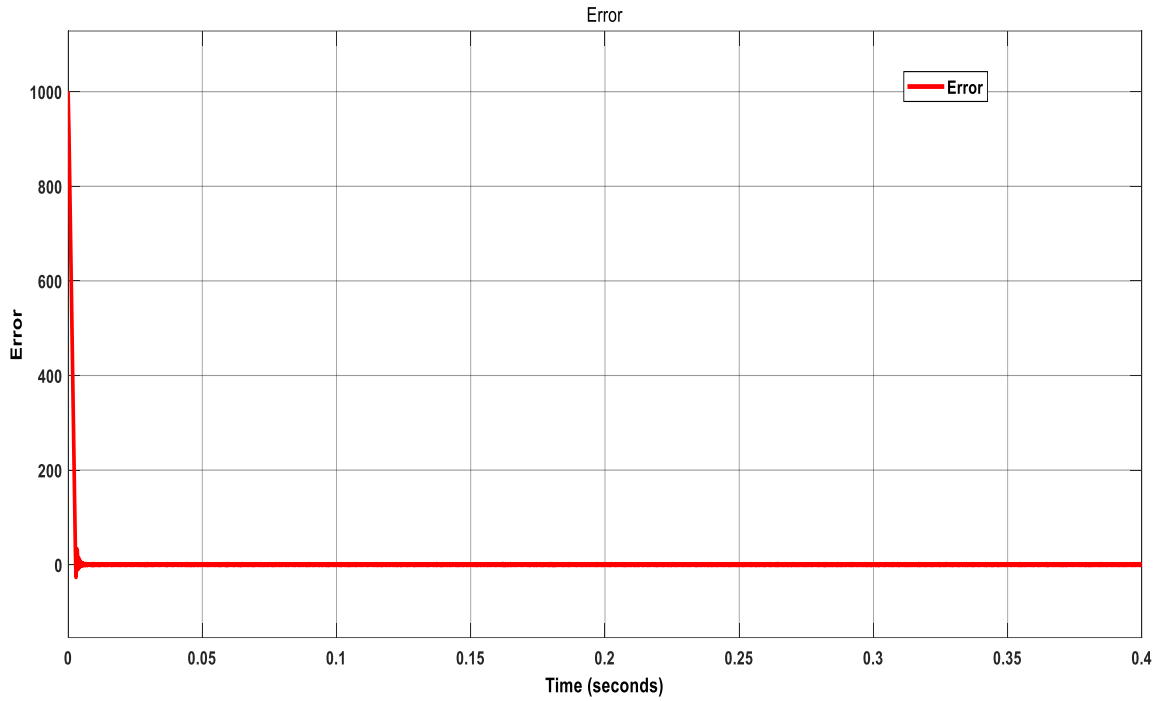

Figure 5.4 Error in the PMSM's actual and reference speeds when there is no load.

The currents produced by the three phase inverter in the three phase stator are another simulation result. An SVPWM block controls this three phase inverter to generate the correct stator current and voltage. As demonstrated in figure 5.5 and with the detail view also given in figure 5.6, For proper rotational flux generation, these three phase currents should have an identical amplitude and a 60° phase shift.

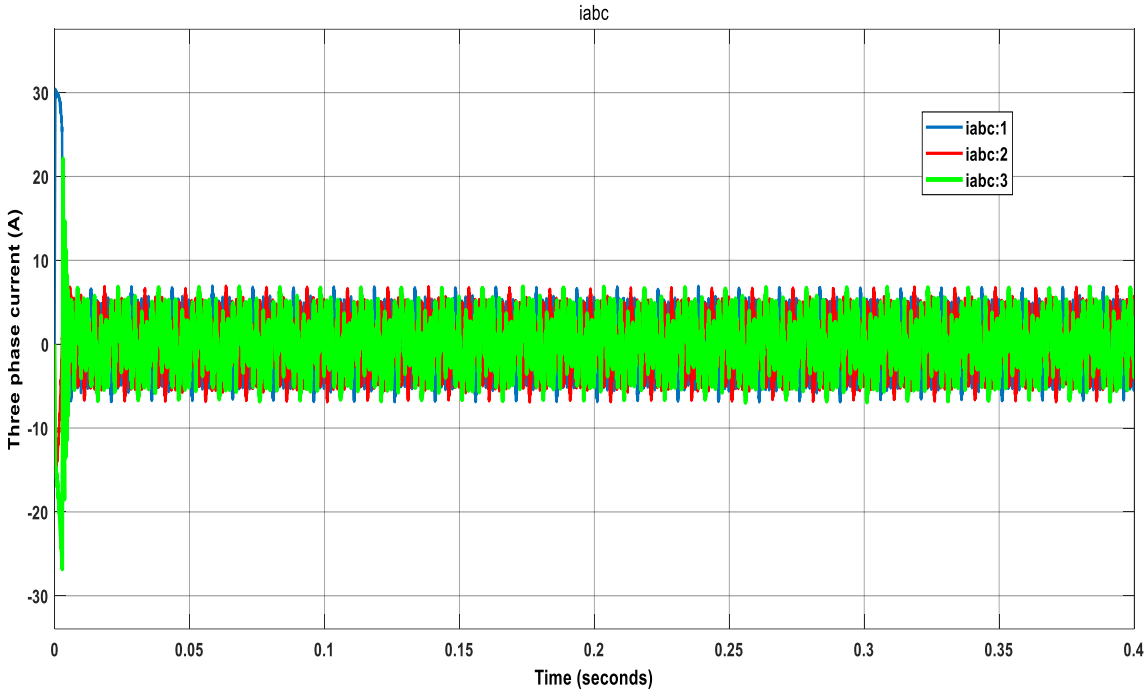

Figure 5.5 During no-load operation, the motor's three phase stator current

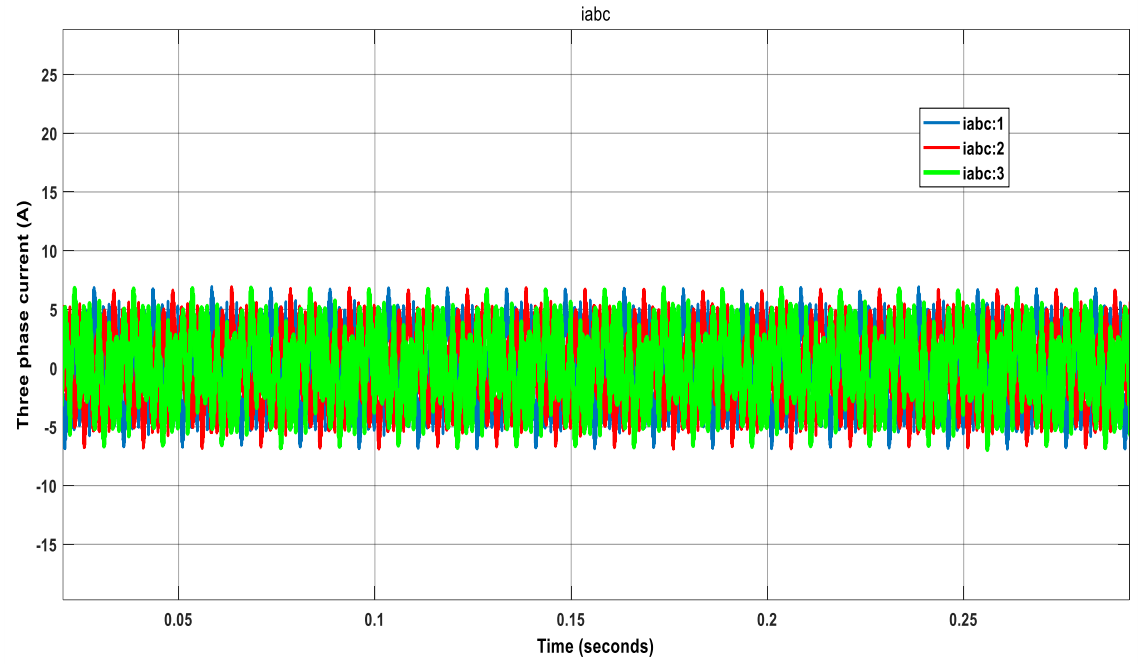

Figure 5.6 At no load, Zoom out on three-phase currents for 0.1 and 0.15 seconds.

As seen in figures 5.5 and 5.6, the correct the value of stator phase current is calculated by excellent correctness. As a result, the scheme is able to give the motor the proper stator voltage.

The motor's produced electromagnetic torque is shown in Figure 5.7 when there is no load. The rotor's acceleration to a constant speed of 1000 rpm is primarily to fault for the starting torque's variation up until 0.00 second. the beginning Comparing to steady-state values, torque is greater at 35.39 Nm. The generated torque, however, drops to virtually zero Nm after 0.00 sec, just enabling for the support of the minimal amount of decrease friction.

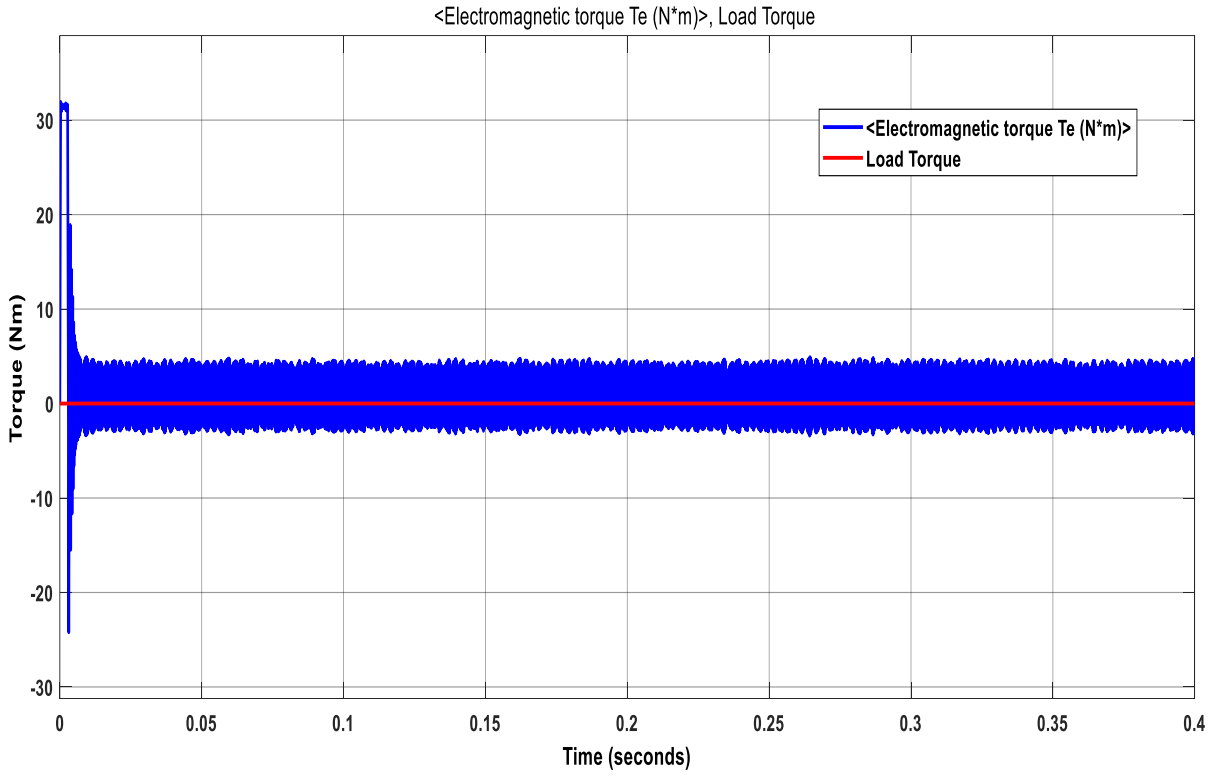

Figure 5.7 Without a load, electromagnetic torque developed.

In Figure 5.8, the fast response follows a specific steps from input 500 rpm to 1000 rpm. The system's fast response prefers a two-step speed level, as seen in the figure. To begin, the 1 000 rpm is the speed setting. immediately the speed changes at y = 0.2 second and stabilizes at 1000 RPM. The system functions better when the motor is step input for the first level, or at 500 rpm, which is slower than the maximum speed, as shown in figure 5.3. This is accurate in terms of settlingtime, rise time, and maximum overshoot. As a result, the system's chattering effect is reduced,shown in the figure.

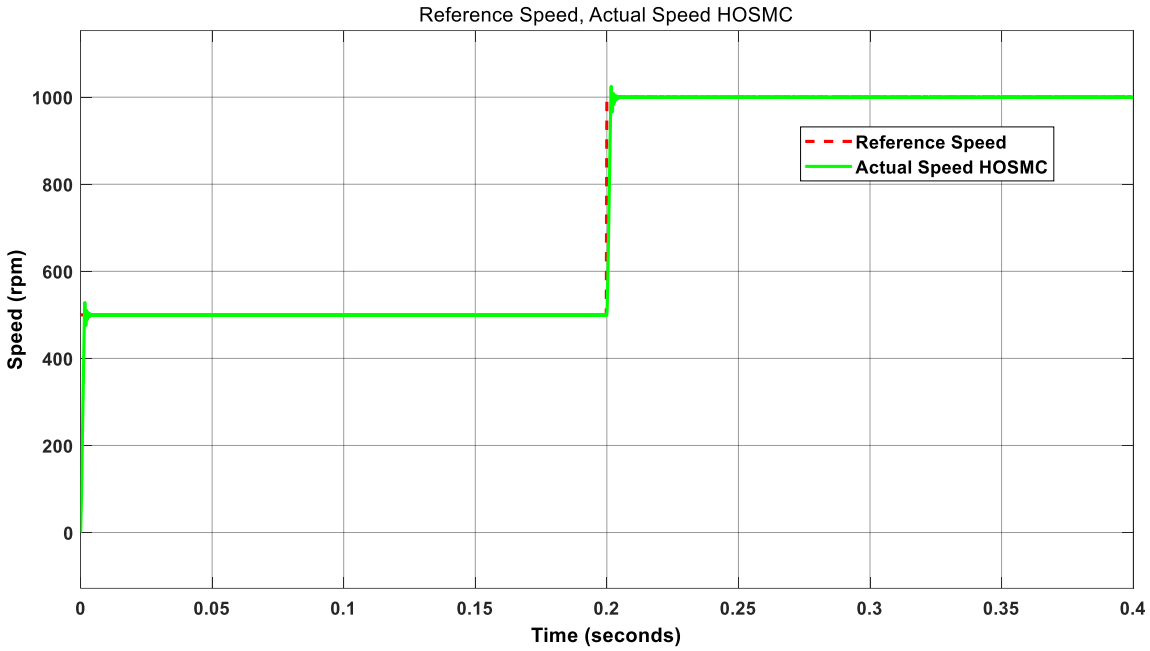

Figure 5.8 Step input response at speeds between 500 and 1000 RPM when there is no load.

Additionally, the device has good speed tracking in both forward and reverse modes while operating. Figure 5.9, which displays the simulation's result when the motor is operating in both forward and reverse direction. at 1000 rpm. When evaluating the performance of this system, we can see that the system works better in the forward condition than in the reverse state the rising time and settling time for some control parameters.

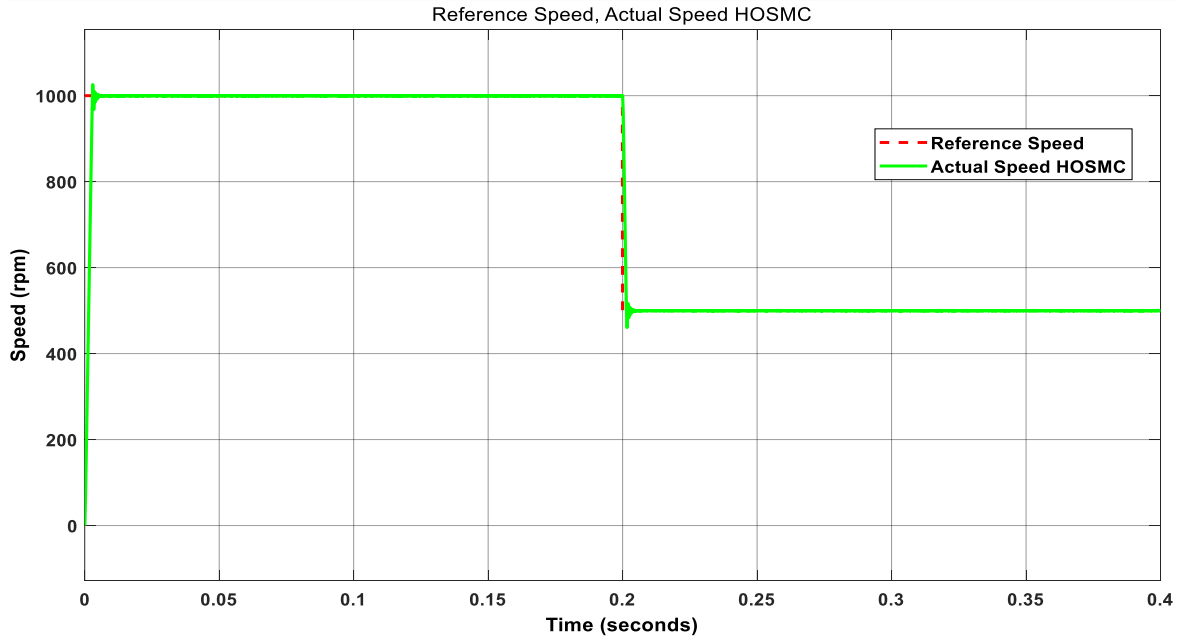

Figure 5.9 Speed response in forward and reverse when there is no load

The system's developed electromagnetic torque under load torque conditions is shown in Figure 5.10 for the system. According to figure 4.7, the produced electromagnetic torque changes in response to the motor's acceleration during transients. On the other hand, the electromagnetic torque takes longer than the no-load conditions 0.057 seconds to reach the steady-state response (10Nm). The advantage of vector control, as mentioned in Chapter 3, is that it uses the stator current to directly regulate the motor torque. Figures 5.10 and 5.11 illustrate how the electromagnetic torque is inversely proportional to the q-axis current. A 10Nm load torque was used during the simulation's execution.

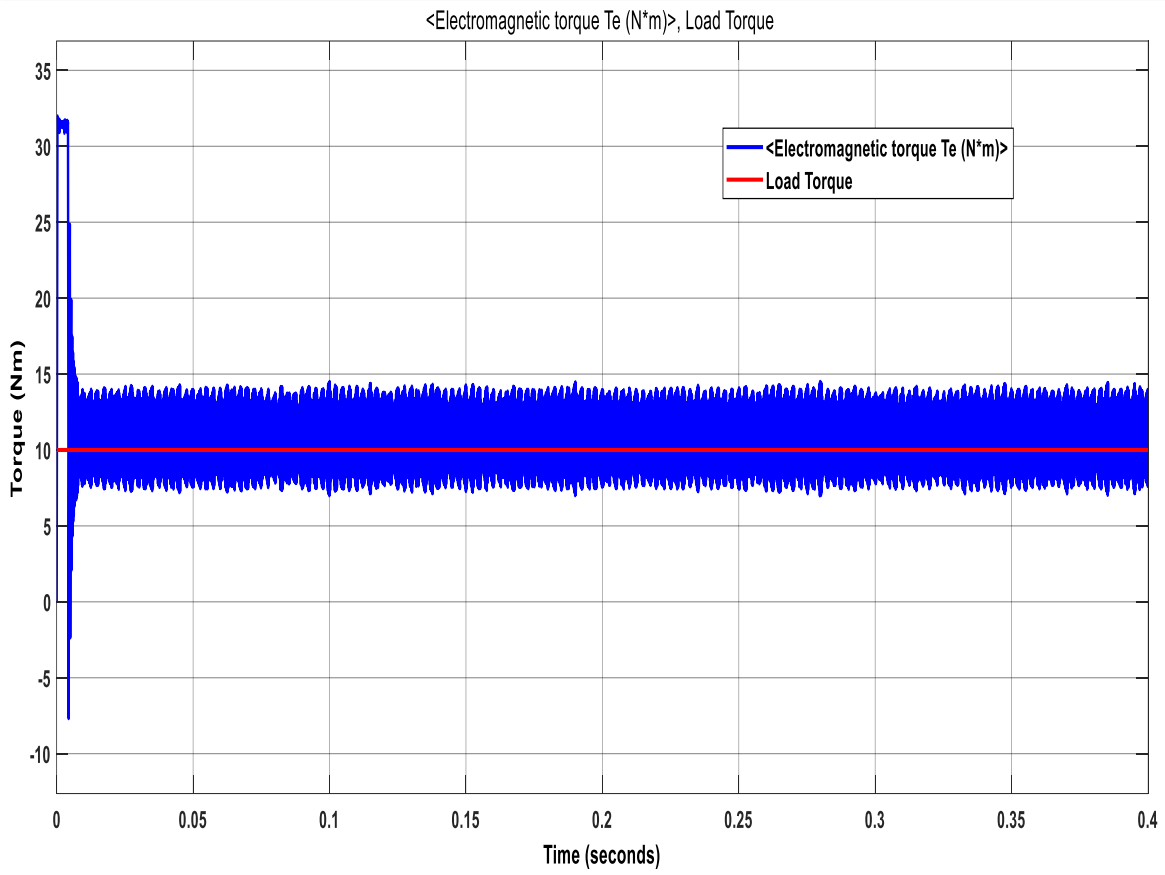

Figure 5.10 developed electromagnetic torque under the condition of a (T1=10 Nm) load torque.

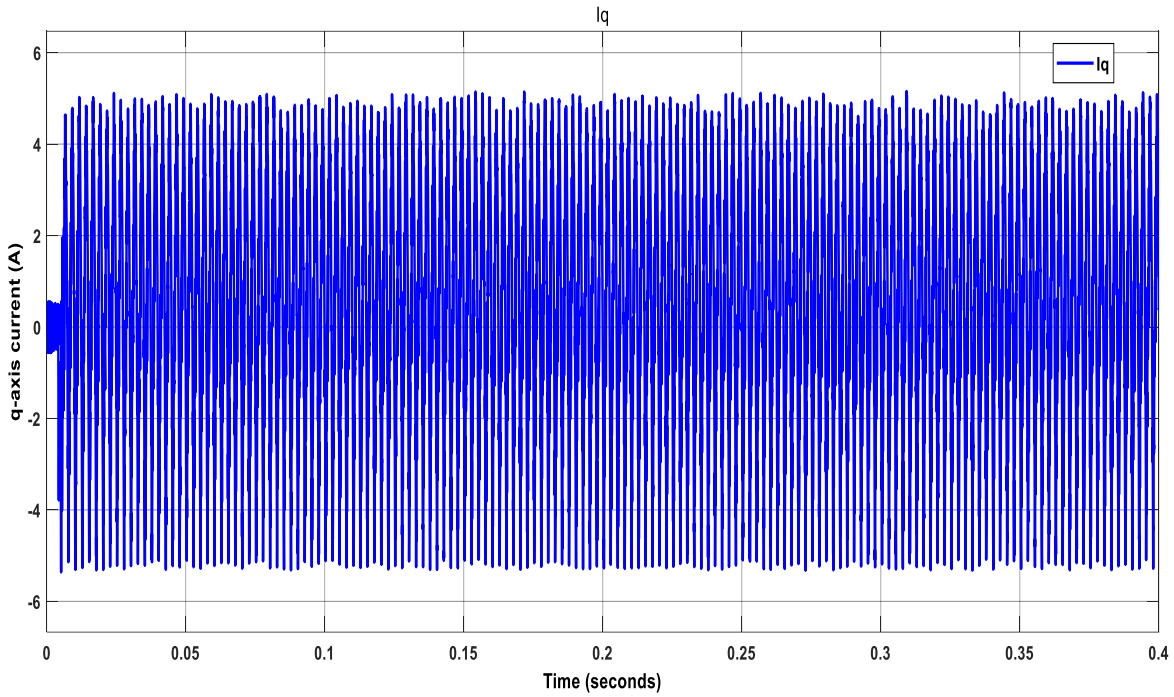

Figure 5.11 The q-axis stator current

Figure 5.12 illustrates the system's speed response at 10Nm torque load. The system also performs well in terms of control parameters.

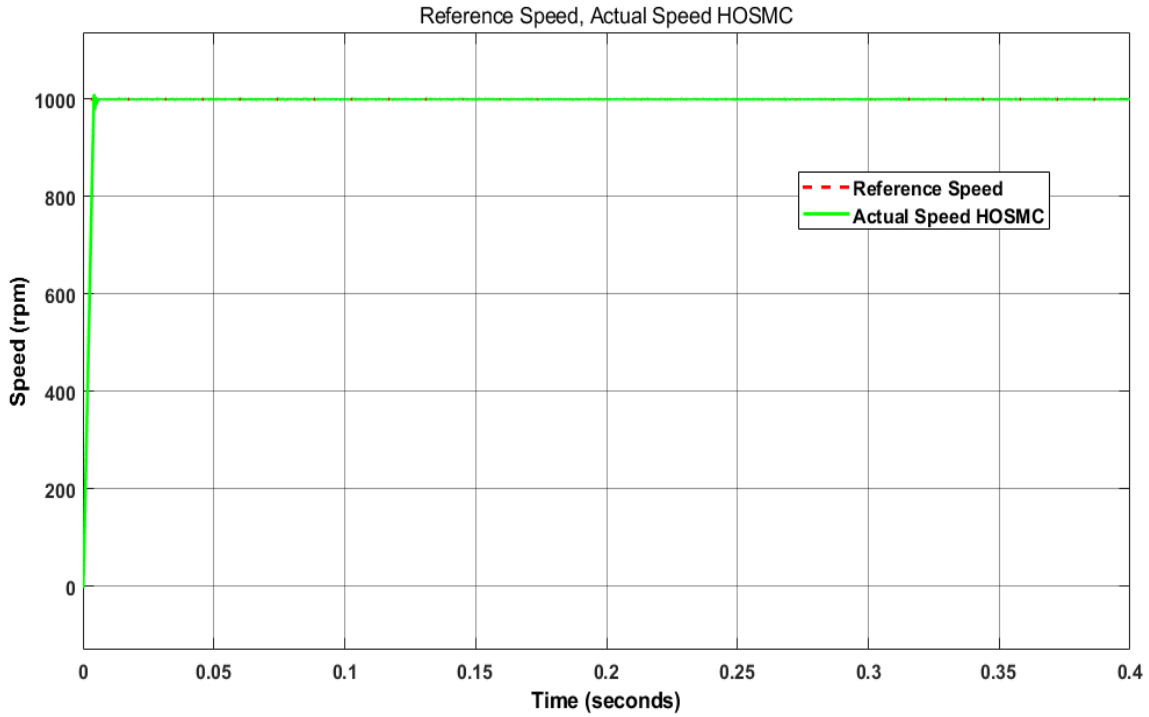

Figure 5.12 The PMSM's response time at 10 Nm of load torque.

Stator phase currents in the system has a good steady-state and transient response when loaded, These properties are showed in figure 5.13 and 5.14.

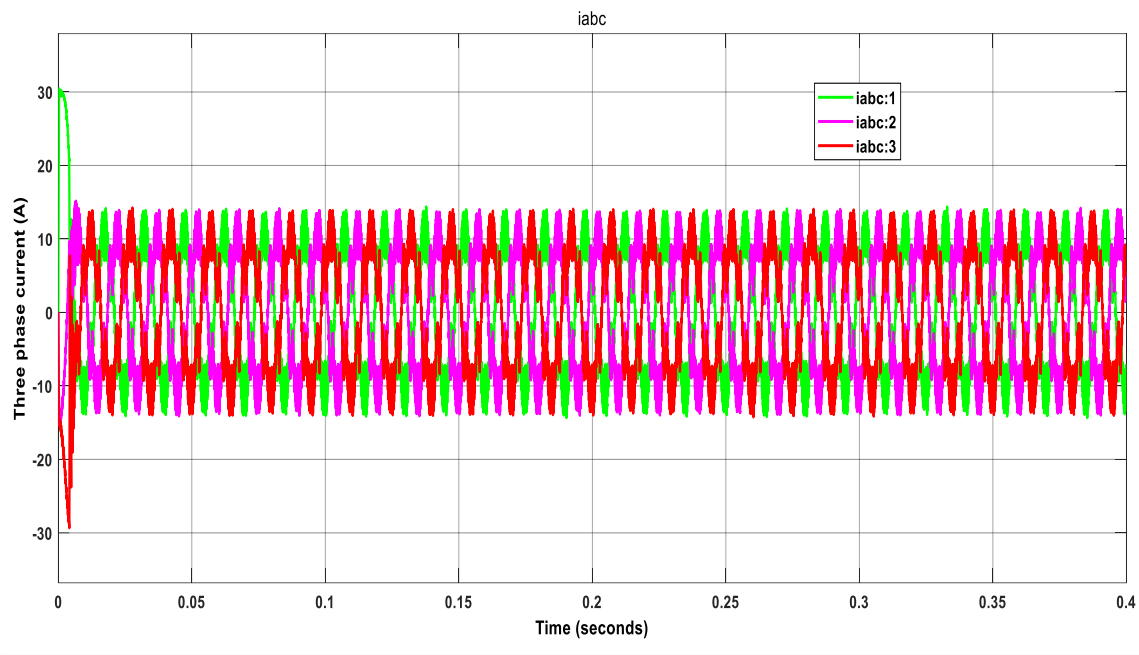

Figure 5.13 Three phase stator current with a 10Nm load torque on the motor

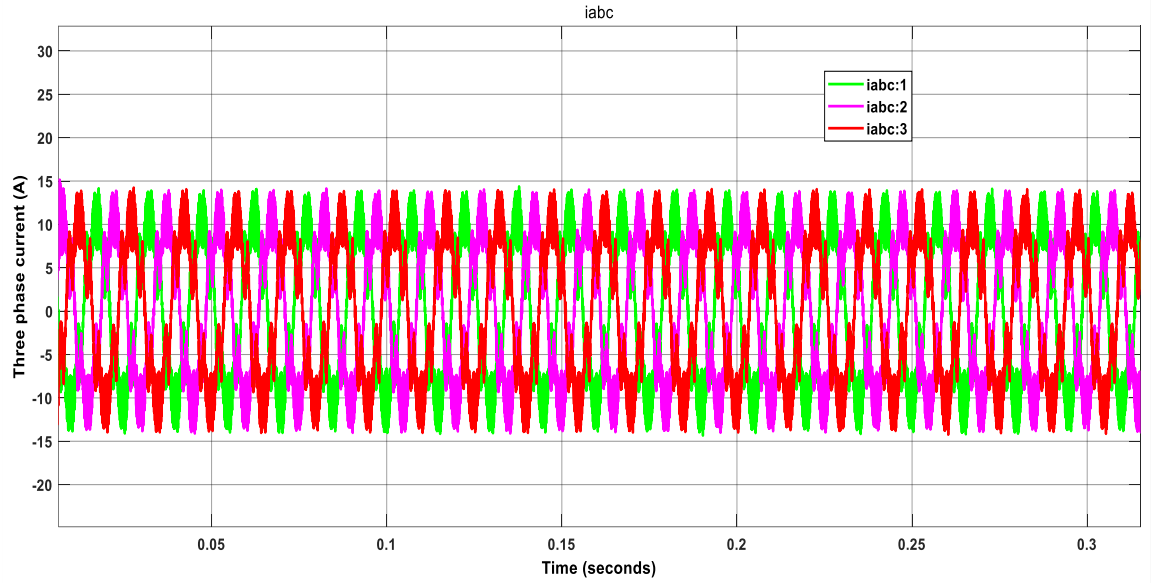

Figure 5.14 At a 10 Nm load condition, in three phase current between 0.00 and 0.05 sec.

Figures 5.15 to 5.17 depict the system's performance as a result of motor parameter variation due to various factors such as temperature. Figures 5.15, 5.16, and 5.17 show the system's speed response while without the load torque the Increases in 50% of the motor stator's inductance, moment of inertia, and resistance their minimal values. These numbers demonstrate the PMSM control system's high performance and reliability. The three graphs

demonstrate how precisely the The specified speed can be adjusted through the use of a permanent magnet synchronous motor.

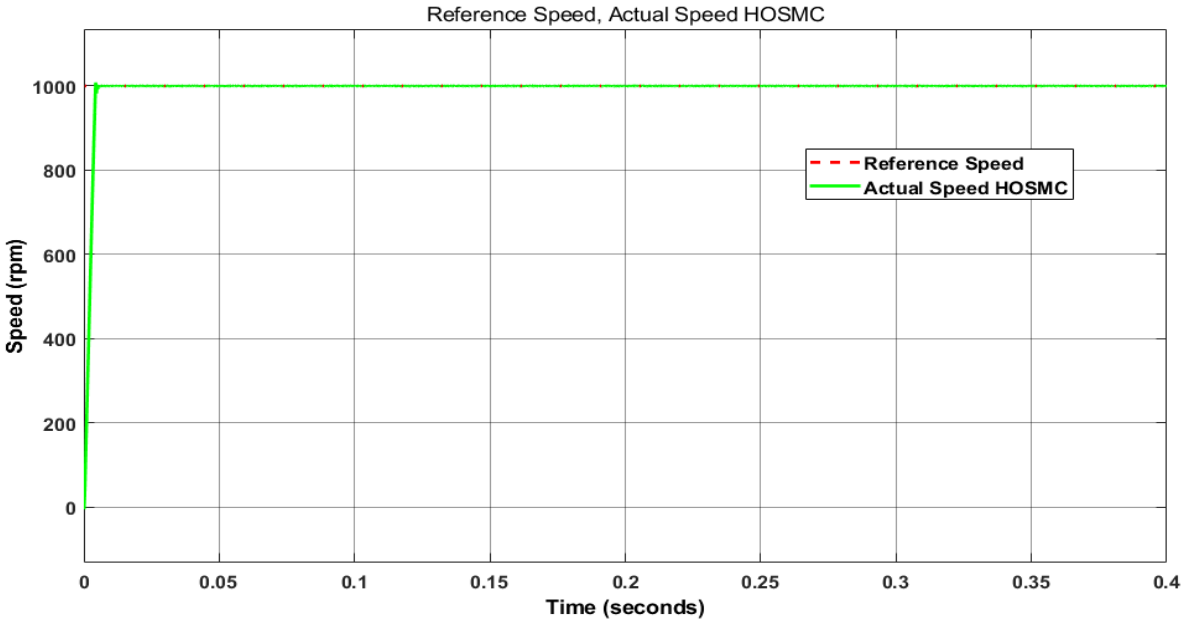

Figure 5.15 Motor speed after a 50% increase in stator resistance.

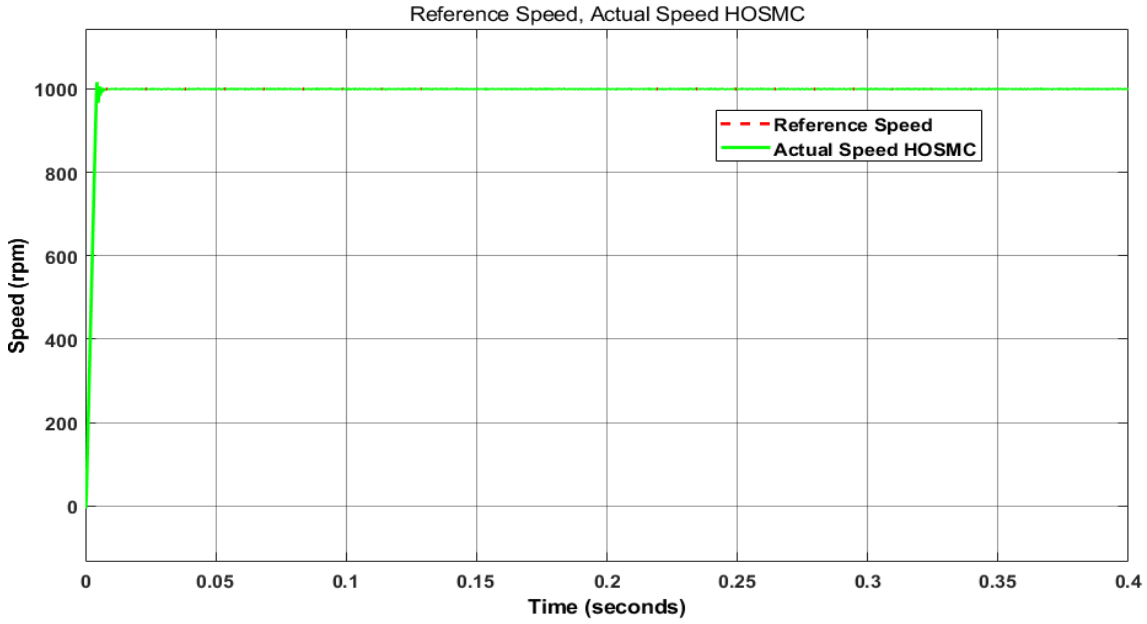

Figure 5.16 Motor speed after a 50% increase in stator inductance.

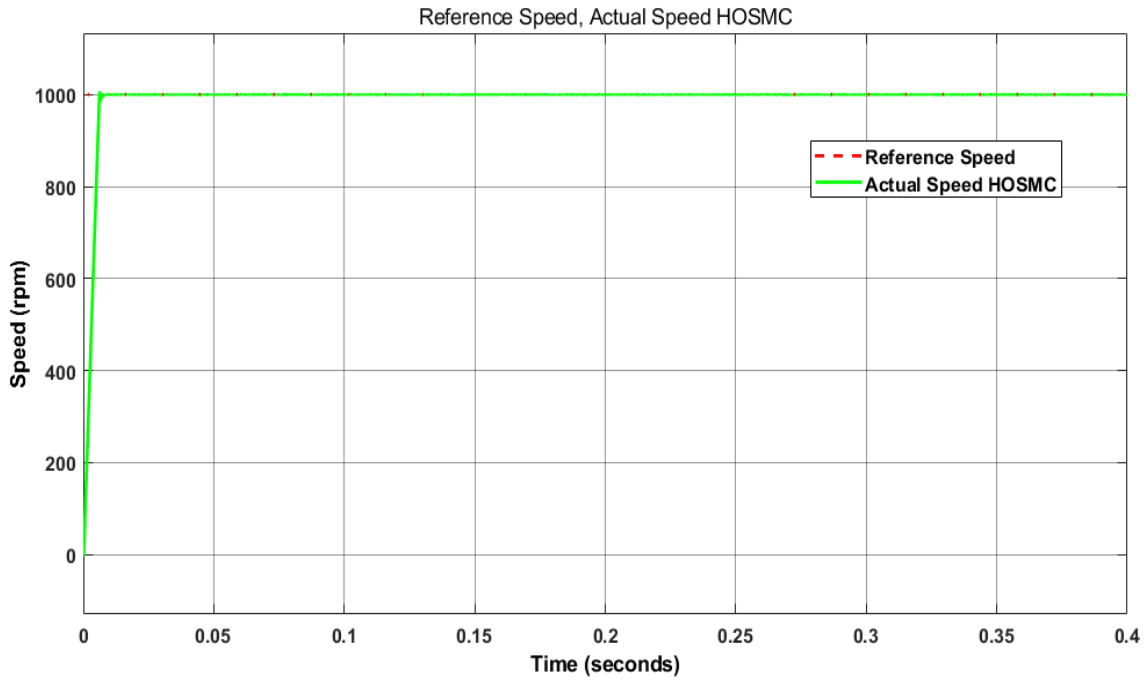

Figure 5.17 Motor speed at a 50% increase in moment of inertia.

In order to verify the correctness of the designed speed controller, the simulation conditions are set as the reference speed Nef=1000 RPM, the initial load torque T_L. = 0 Nm and the load torque T_L= 10N at times 0.2sec, the simulation results are shown in figures 5.18.

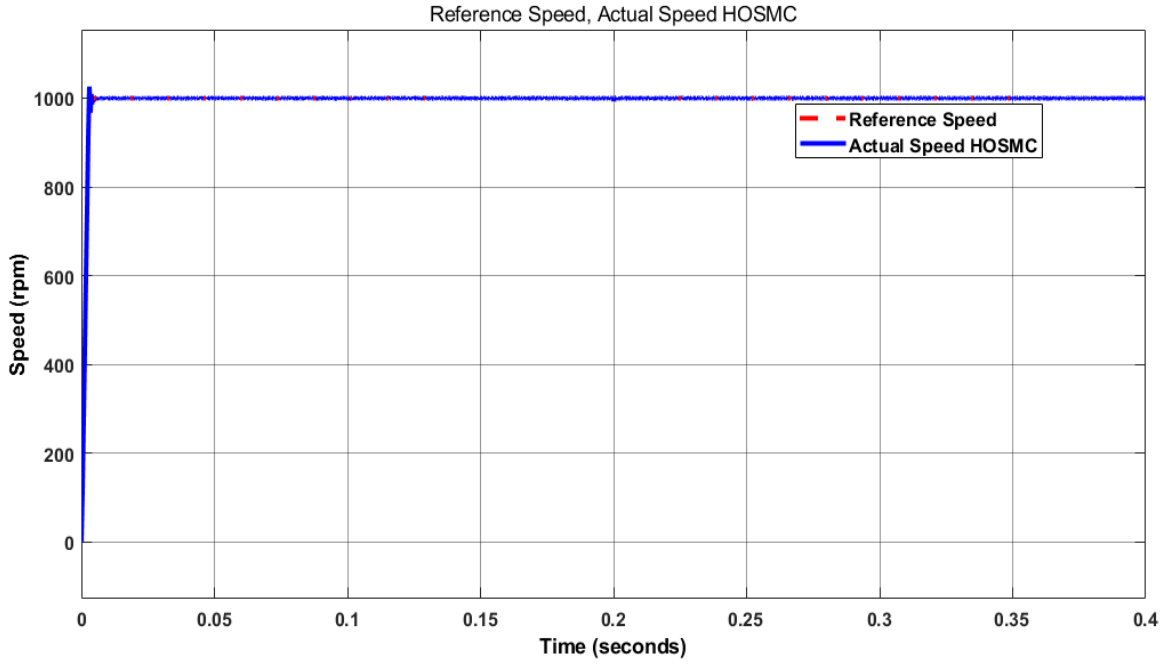

(a) Speed Change Curve

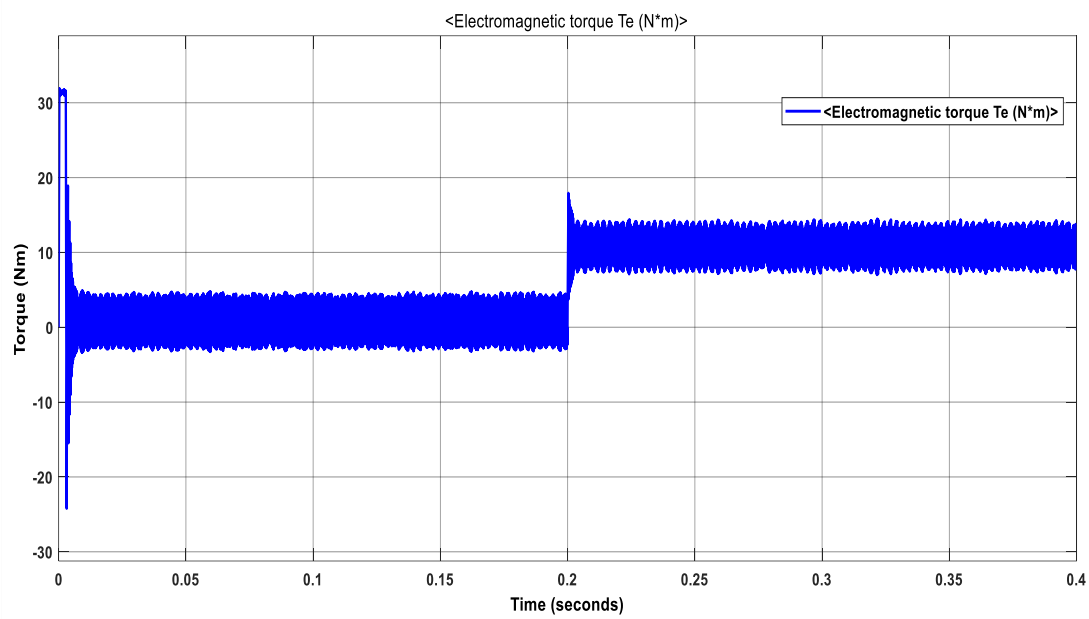

(b) Electromagnetic torque and change curve

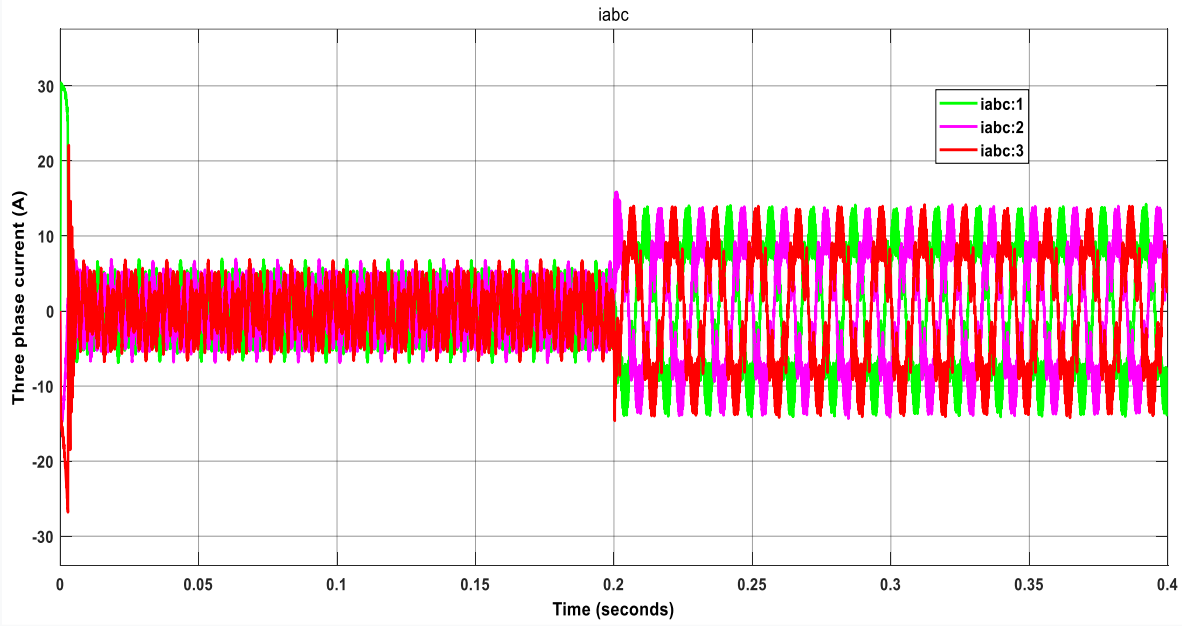

phase current sound change curve

Figure 5.18 Simulation resultsof PMSM Vector Control System based on HOSMC

The Simulation result show that when the reference speed is 1000rpm, the motor starts from zero speed. Although the motor speed overshoots at first, it still has a fast dynamic response speed at t=0.2 sec sudden load torque T_L =10Nm, the motor can also quickly recover to the specified reference speed, indicating that the set. The high order sliding mode speed controller

has good dynamic performance and anti-disturbance capability, allowing it to meet actual motor controllability.

5.3 Simulation Result and Analysis of SMC

The sliding mode controller in this work was built using a HOSMC sliding surface. SMC sliding surface performance is contrasted with that of the suggested sliding surface design. Similar to this, a reference 500rpm speed and a 10 Nm load torque were applied at t = 0.5 s. Figure 5.19 shows that compared to HOSMC with SMC sliding surface, HOSMC with SMC sliding surface produced a better speed response with nearly 19 times less overshoot. HOSMC had a speed loss of 4 % when a load torque of 10 Nm was applied, which is 2.8 % more than the speed drop of an SMC system. The SMC system returned to reference speed after the speed drop after almost 0.01 s, whereas the HOSMC system did so one fifth more quickly. The performance of HOSMC stood out in trms of torque ripple, with the resulting ripple being half that of SMC.

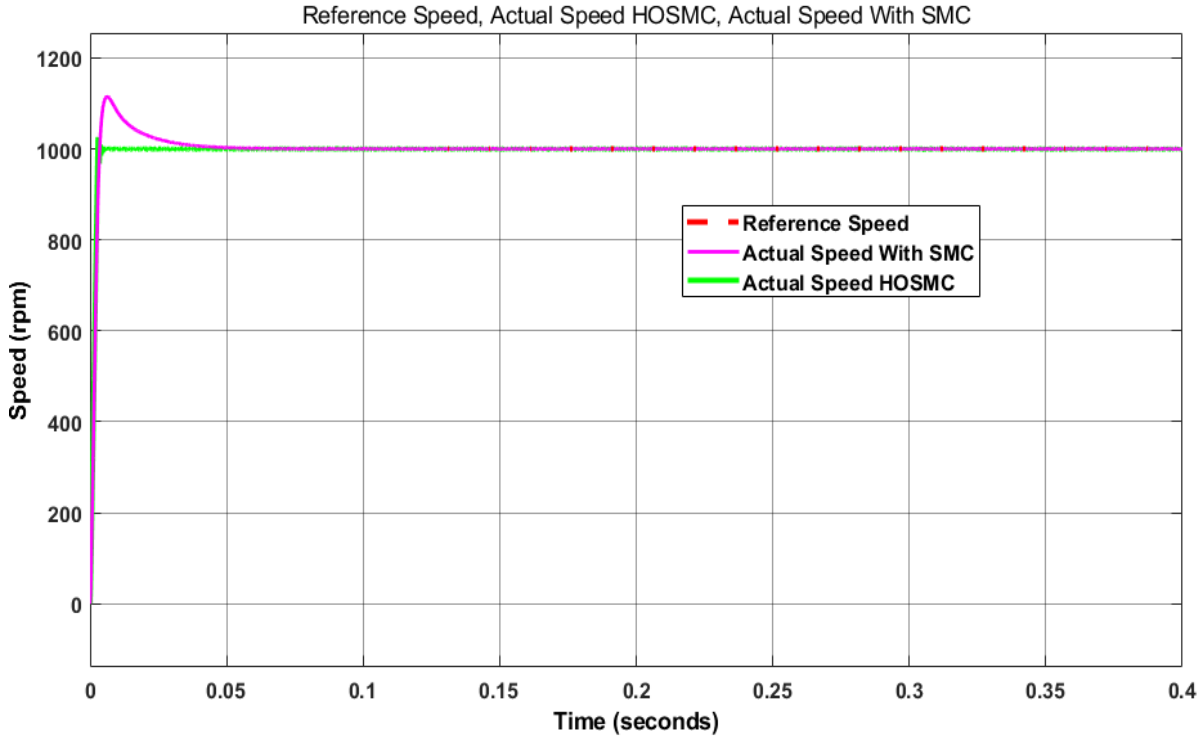

Figure 5.19 SMC and HOSMC speed response at 1000 rpm with no load

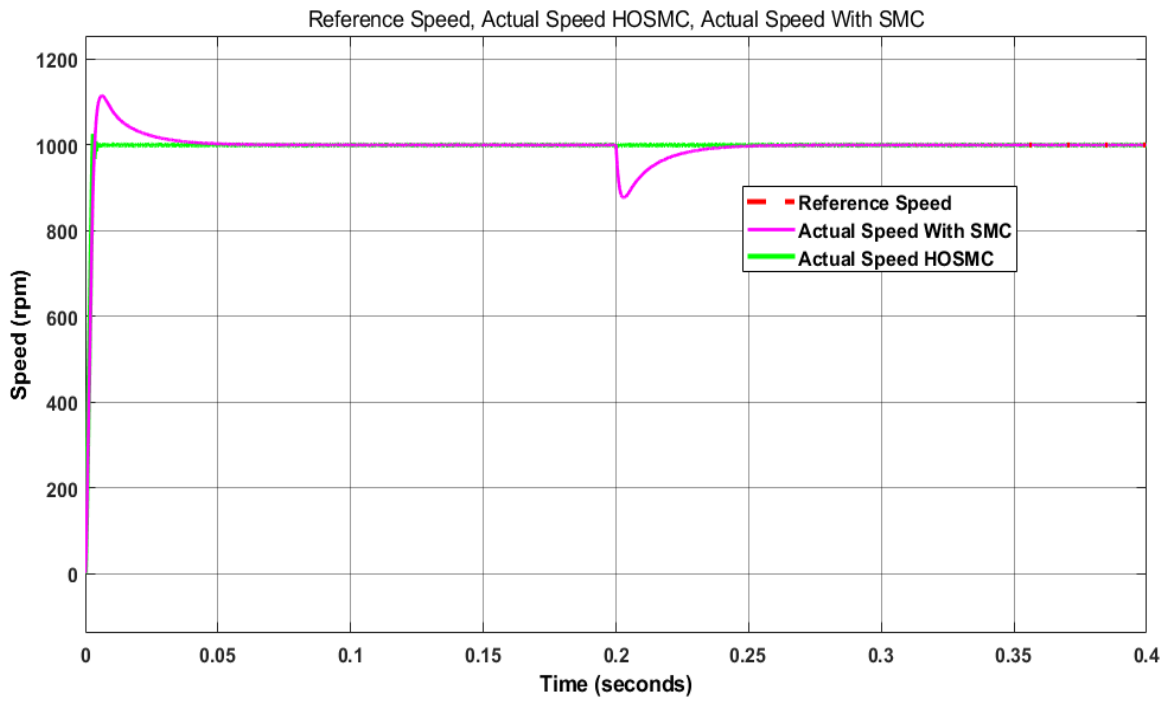

figure 5.20 SMC and HOSMC speed responses for 1000 rpm at 0 to 10 Nm of load torque

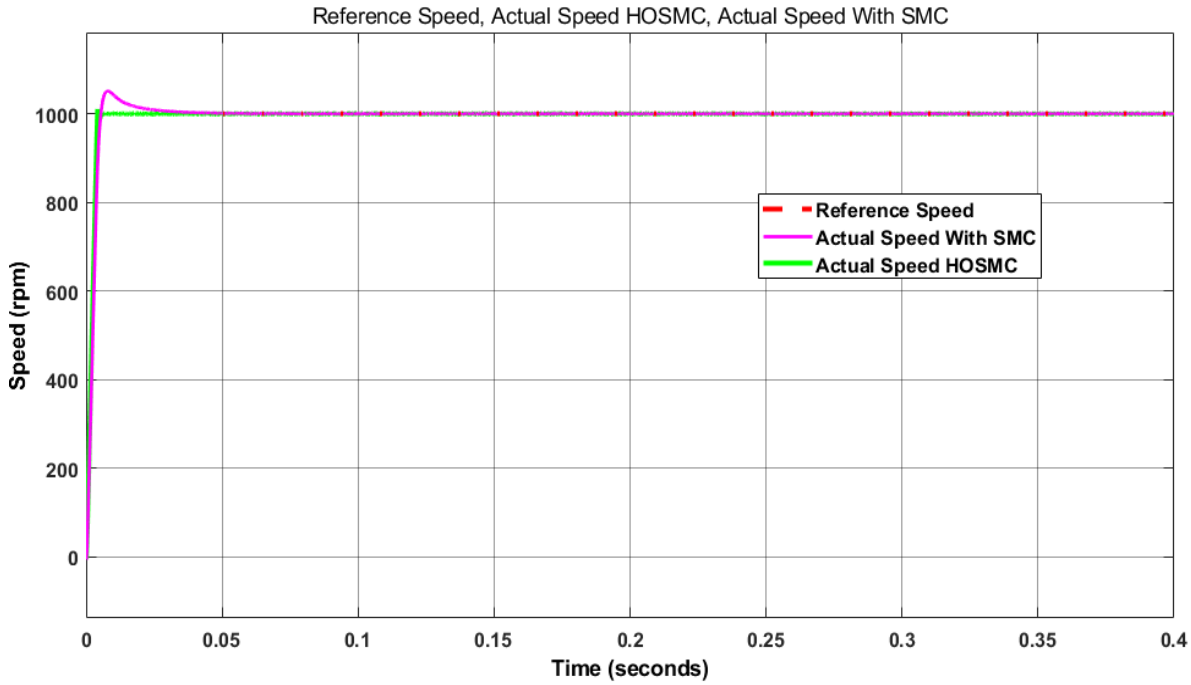

Figure 5.21 Speed response of SMC and HOSMC for 1000rpm at 10Nm load torque

Table 5.1 SMC and HOSMC Performance Comparison

No.	Performance parameters	SMC	HOSMC
1	Overshoot at 1000rpm, applying no load torque	11.798%	2.577%
2	settling period (t_s) at 1000rpm, no load torque applied	-	2.065msec
3	Rise time at 1000rpm, noload torque applied	2.439msec	2.152msec
4	Overshoot at 1000rpm, 10 N.m Load torque applied	4.737%	1.531%
5	Settling time at 1000rpm, 10N.m Load torque applied	11.995mdec	1.926msec
6	Rise time at 1000rpm, 10Nm load torque applied	3.661msec	3.175msec

The simulation results show that when the motor accelerates from zero to the reference speed of 1000RPM, the speed estimation error has greater value in the rising speed at this point, but as the speed increases and after the stable operation, the speed estimation is incorrect. The difference becomes very small, as does the rotor position estimation error. This demonstrates that by selecting the appropriate control. This is due to a change in the testing profile and filter tuning for a lower speed operation condition.

5.4 Results Analysis

The first order sliding mode controller was designed using the sigmoid function. Because heavy filtering was discovered to be necessary, the system's complexity was increased.a high order sliding mode controller was implemented to address this issue. Using an integral term in the sliding law improved the controller's direct output signal (e.g., reduced chattering), requiring less filtering, as demonstrated in research papers. The controller parameters were calculated using model parameters, and it is important to note that errors due to parameter uncertainties will always exist. The problem was revisited, and it was determined that implementing a voltage error compensator would result in a significant improvement after trial tests and additional analysis. The compensator was then designed using the device's dead-time, switching on and off time, and voltage loss. The dead-time was discovered to have the greatest influence on the calculation. Furthermore, the other parameters are unknown with certainty. For these reasons, the compensator's final version only used the dead-time. However, it was not used in any of the simulations. The simulations revealed that the transient response of the systems is rather slow. A load torque compensator was required. Even with simple feed forward load torque compensation, the transient response was significantly improved.

Throughout all simulation tests, the system was started from a standstill using regular, sensored FOC. Across all estimators, the filter parameters were kept constant. This means they were not tuned specifically for an estimator. This was done in order to reduce the number of variables that existed between systems.

5.5 Results summary

The simulation's outcomes were generally encouraging. For a PMSM, the system achieves reliable control despite the uncertainty in the internal parameters and the unidentified external load torque disturbance. The simulation's results show that for a given reference input, our controller works well in relation to maximum, settling time and steady-state error, rising time, and overshoot. The motor has good speed tracking, according to the simulation findings. As illustrated in Figures 5.5 and 5.18, a three phase inverter controlled by the SVPWM algorithm performs well. The generated current has an equal magnitude and a phase shift of 60 degrees theorem of high order sliding mode controls and nonlinear system control theory are the main topics of this thesis. It is challenging to create in practice an accurate approximation of the technical requirements for precise feedback linearization technology for nonlinear systems. The resilience of conventional switching to sliding mode control, which is subject to ambiguous systemic model parameters or unidentified external disturbances, is maintained by technology for high order sliding mode control opposed to traditional sliding mode control, the chattering phenomena caused by discontinuous discrete control is transferred to a low order sliding surface is a result of a higher order sliding surface to improving control precision and remove chattering. These findings indicate that the FOC or vector control algorithm functions effectively.

CHAPTER SIX

CONCLUSION AND RECOMMENDATION

6.1Conclusions

The use of a high order sliding mode controllerto control the synchronous motor's permanent magnet speed was in this thesis. A nonlinear, time-varying MIMO complex system, the PMSM system. For higher degrees of accuracy, controlling the speed of a PMSM with an SMC is insufficient. Consequently, A control with the purpose of a high order sliding mode is to improve reaction and produce positive results under all circumstances while also reducing chattering and assuring system durability. high order sliding mode control, as a result, has not only a significant control of complicated, nonlinear systems that change as time passes, then it similarly maintains the strength of various control methods that are robust to uncertainty systematic model parameters and unidentified external disturbances.High order sliding mode control, as opposed to conventional sliding mode control, eliminates chattering by using a difference of the sliding mode variable at a high order. The Matlab/Simulink software package was used to simulate the entire system. The entire syste is simulated, including the controller,various coordinate transformations, the inverter, and the PMSM. At no load and loaded torque conditions, Three phase stator currents, produced electromagnetic torque, and system performance and speed responsiveness were all measured. To improve system performance and response time, plant factors like moment of inertia, inductance, and stator resistance can be adjusted. The system's speed response in reverse, forward, and step input at any given time.

The simulations results demonstrate that using a HOSM controller to regulate the speed of a PMSM has good performance as, as demonstrated in figures 5.3 and 5.14, The system recovers fully from all overshoot and settling time is less than one second the abovementioned modes.As a result, the system is capable of operating in a wide range of load torque and environmental conditions. Significant robustness tests are performed, and simulation results demonstrate the efficiency of the controller scheme.

6.2 Recommendation and Future work

There are still several important topics that need to be investigated and researched in regard to the high order sliding mode control of nonlinear systems covered in this thesis.

1. The focus of this paper is the nonlinear system's Control with affine and matching high order sliding mode. It doesn't study nonlinear systems that aren't affine or that don't match.which is a focus of nonlinear sliding mode control research.
2. Because of the theory's limitations, It has not yet been possible to generalize the use of the smooth control rule and a quasi-continuous high order sliding mode control method. Its major goal is to minimize the quantity of discrete sign function components in the control legislation. As the denominator of the control law approaches zero, however, doubtful items may occur for some particular actual systems. The issue that has to be resolved in the future is that this concept is still very helpful.
3. For nonlinear permanent magnet synchronous motors, It is widely known that state estimation and estimation of external disturbances can be actually achieved by sliding mode control using a differentiator. In light of this, it ought should be feasible to find system parameters online. The simulation showed that more precise identification of stator resistances and motor flux values is possible. Inductance is certainly a more significant factor when it comes to motors. However, the results of several simulations' inductance identification were not adequate. The reason for this is that although the unit of electrical inductance is millihenry under normal circumstances, a zero-zero occurrence happens when we estimate it using the sliding mode variable and pertinent state variables. The molecular and denominator of the inductance also approach zero as the sliding variable approaches zero over a finite period of time.. As a result, the method's identification reliability requires further investigation.
4. High order sliding mode control minimizes chattering and has improved control accuracy while retaining traditional sliding mode control's robustness. It does, however, seek high order derivatives under a given reference value, which is a roadblock. As a result, in the time domain, a given function must be continuously differentiable everywhere. In practice, the system is far harsher. As a result, one of the most important research topics for How is by high order sliding mode control to relax the operating conditions.

REFERENCE

[1] F. M. Zaihidee, S. Mekhilef, and M. Mubin, "Robust speed control of pmsm using sliding mode control (smc)-a review," *Energies*, vol. 12, no. 9, 2019, doi: 10.3390/en12091669.

[2] S. Chi, Z. Zhang, and L. Xu, "Sliding-mode sensorless control of direct-drive PM synchronous motors for washing machine applications," *IEEE Trans. Ind. Appl.*, vol. 45, no. 2, pp. 582–590, 2009, doi: 10.1109/TIA.2009.2013545.

[3] J. Huang, H. Li, F. Teng, and D. Liu, "Fractional order sliding mode controller for the speed control of a permanent magnet synchronous motor," *Proc. 2012 24th Chinese Control Decis. Conf. CCDC 2012*, pp. 1203–1208, 2012, doi: 10.1109/CCDC.2012.6244192.

[4] Y. Shtessel, C. Edwards, and L. Fridman, *Sliding Mode Control and Observation, Series: Control Engineering*, vol. 10. 2016. [Online]. Available: http://www.springer.com/gp/book/9780817648923#reviews

[5] W. Dai and H. Li, "Study of direct torque control (DTC) system of permanent magnet synchronous motor based on DSP," *ICEMS 2001 - Proc. 5th Int. Conf. Electr. Mach. Syst.*, vol. 2, pp. 921–924, 2001, doi: 10.1109/ICEMS.2001.971829.

[6] M. Štulrajter, V. Hrabovcová, and M. Franko, "Permanent magnets synchronous motor control theory," *J. Electr. Eng.*, vol. 58, no. 2, pp. 79–84, 2007.

[7] C. Zhou, Z. Zhou, W. Tang, Z. Yu, and X. Sun, "Improved Sliding-Mode Observer for Position Sensorless Control of PMSM," *Proc. 2018 Chinese Autom. Congr. CAC 2018*, no. 3, pp. 2374–2378, 2019, doi: 10.1109/CAC.2018.8623482.

[8] M. Legesse, "Speed Control of Vector Controlled PMSM Drive using Fuzzy Logic-PI Controller," *Addis Ababa Inst. Technol. (AAiT), August*, vol. 201, 2011.

[9] Y. Huangfu, S. Laghrouche, W. Liu, and A. Miraoui, "A chattering avoidance sliding mode control for PMSM drive," *2010 8th IEEE Int. Conf. Control Autom. ICCA 2010*, no. 3, pp. 2082–2085, 2010, doi: 10.1109/ICCA.2010.5524303.

[10] Z. Ding, G. Wei, and X. Ding, "Speed identification and control for permanent magnet synchronous motor via sliding mode approach," *Syst. Sci. Control Eng.*, vol. 2, no. 1, pp. 161–167, 2014, doi: 10.1080/21642583.2014.886974.

[11] M. Ezzat, J. De Leon, N. Gonzalez, and A. Glumineau, “Observer-controller scheme using high order sliding mode techniques for sensorless speed control of permanent magnet synchronous motor,” *Proc. IEEE Conf. Decis. Control*, pp. 4012–4017, 2010, doi: 10.1109/CDC.2010.5717365.

[12] H. Yi-geng, “A Dissertation for the Degree of Philosophy Doctor Research of Nonlinear System High Order Sliding Mode Control and its Applications for PMSM,” 2010.

[13] R. Delpoux and T. Floquet, “High-order sliding mode control for sensorless trajectory tracking of a PMSM,” *Int. J. Control*, vol. 87, no. 10, pp. 2140–2155, 2014, doi: 10.1080/00207179.2014.903563.

[14] L. Sun, X. Zhang, L. Sun, and K. Zhao, “Nonlinear speed control for PMSM system using sliding-mode control and disturbance compensation techniques,” *IEEE Trans. Power Electron.*, vol. 28, no. 3, pp. 1358–1365, 2013, doi: 10.1109/TPEL.2012.2206610.

[15] Z. Xu and M. F. Rahman, “Comparison of a sliding observer and a Kalman filter for direct-torque-controlled IPM synchronous motor drives,” *IEEE Trans. Ind. Electron.*, vol. 59, no. 11, pp. 4179–4188, 2012, doi: 10.1109/TIE.2012.2188252.

[16] J. Beerten, S. Member, J. Verveckken, and J. D. Member, “Torque Ripple Reduction,” *2017 IEEE Int. Conf. Power, Control. Signals Instrum. Eng.*, vol. 57, no. c, pp. 1–9, 2009.

[17] M. Ruderman, A. Ruderman, and T. Bertram, “Observer-based compensation of additive periodic torque disturbances in permanent magnet motors,” *IEEE Trans. Ind. Informatics*, vol. 9, no. 2, pp. 1130–1138, 2013, doi: 10.1109/TII.2012.2222040.

[18] H. Kim, J. Son, and J. Lee, “A high-speed sliding-mode observer for the sensorless speed control of a PMSM,” *IEEE Trans. Ind. Electron.*, vol. 58, no. 9, pp. 4069–4077, 2011, doi: 10.1109/TIE.2010.2098357.

[19] P. Liu, “A time-domain panel method for oscillating propulsors with both spanwise and chordwise flexibility,” 1996. [Online]. Available: http://www.engr.mun.ca/~pliu/Phd.zip

[20] S. Liu, J. Wang, and Z. Zheng, “Research on PMSM Speed Control System Based on Adaptive Fuzzy Control,” *J. Phys. Conf. Ser.*, vol. 1732, no. 1, 2021, doi: 10.1088/1742-6596/1732/1/012156.

[21] E. Ojionuka, I. Chinaeke-Ogbuka, C. Ogbuka, and C. Nwosu, “A simplified sensorless speed control of permanent magnet synchronous motor using model reference adaptive system,” *J. Electr. Eng.*, vol. 70, no. 6, pp. 473–479, 2020, doi: 10.2478/jee-2019-0080.

[22] R. Mustafa, Z. Ibrahim, and J. M. Lazi, “Sensorless adaptive speed control for PMSM drives,” *PEOCO 2010 - 4th Int. Power Eng. Optim. Conf. Progr. Abstr.*, no. June, pp. 511–516, 2010, doi: 10.1109/PEOCO.2010.5559258.

[23] J. Zhang and T. Sun, “Parameters Identification of Air-Condition Compressor Driven by Motor Using the Least Squares Method,” *Proc. - 5th Int. Conf. Control Sci. Syst. Eng. ICCSSE 2019*, vol. 1, no. 3, pp. 110–114, 2019, doi: 10.1109/ICCSSE.2019.00029.

[24] D. Vindel, S. Haghbin, A. Rabiei, O. Carlson, and R. Ghorbani, “Field-oriented control of a PMSM drive system using the dSPACE controller,” *2012 IEEE Int. Electr. Veh. Conf. IEVC 2012*, 2012, doi: 10.1109/IEVC.2012.6183206.

[25] A. Levant, “Quasi-continuous high-order sliding-mode controllers,” *IEEE Trans. Automat. Contr.*, vol. 50, no. 11, pp. 1812–1816, 2005, doi: 10.1109/TAC.2005.858646.

[26] D. Liang, J. Li, R. Qu, and W. Kong, “Adaptive second-order sliding-mode observer for PMSM sensorless control considering VSI Nonlinearity,” *IEEE Trans. Power Electron.*, vol. 33, no. 10, pp. 8994–9004, 2018, doi: 10.1109/TPEL.2017.2783920.

[27] J. W. Choi and S. K. Sul, “Inverter output voltage synthesis using novel dead time compensation,” *IEEE Trans. Power Electron.*, vol. 11, no. 2, pp. 221–227, 1996, doi: 10.1109/63.486169.

[28] O. P. Drives, A. R. Mu, and T. A. Lipo, “On-Line Dead-Time Compensation Technique for,” *Trans. Power Electron.*, vol. 14, no. 4, pp. 683–689, 1999.

[29] E. Gruys, “Bildbericht Nr. 17. Magentorsion bei einem Schwein,” *Deutsche Tierarztliche Wochenschrift*, vol. 81, no. 17. p. 411, 1974.

[30] L. A. Pittorino, J. A. du Toit, and J. H. R. Enslin, “Evaluation of converter topologies and controllers for power quality compensators under unbalanced conditions,” *PESC Rec. - IEEE Annu. Power Electron. Spec. Conf.*, vol. 2, pp. 1127–1133, 1997, doi: 10.1109/pesc.1997.616890.

APPENDIX - A

PMSM PARAMETERS

Table A1.1 PMSM Motor Parameters

Parameter	values	Parameter	values
Number of Poles (P_n)	4	Friction Coefficient (B)	0.008Nms
Stator Inductances (L_d and L_q)	$8.5x10^{-3}$H	rotor inertia (J)	0.003JKgm²
Stator resistance (R)	2.875	rotor flux linkage	0.175 Vs

APPENDIX - B

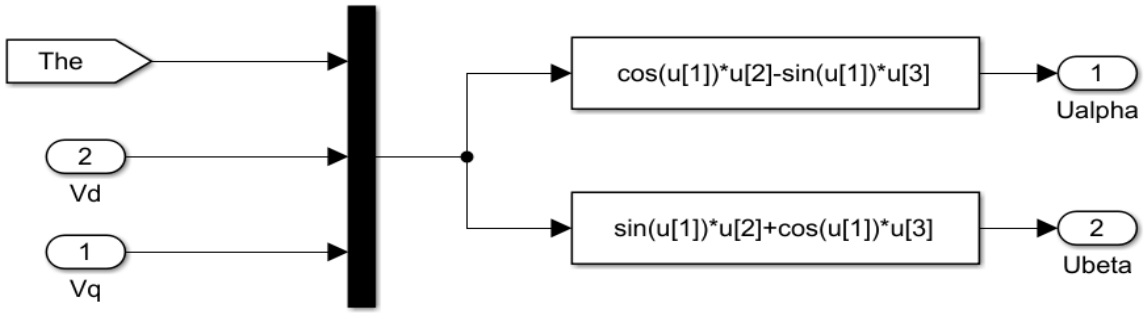

Figure B1.1: anti park

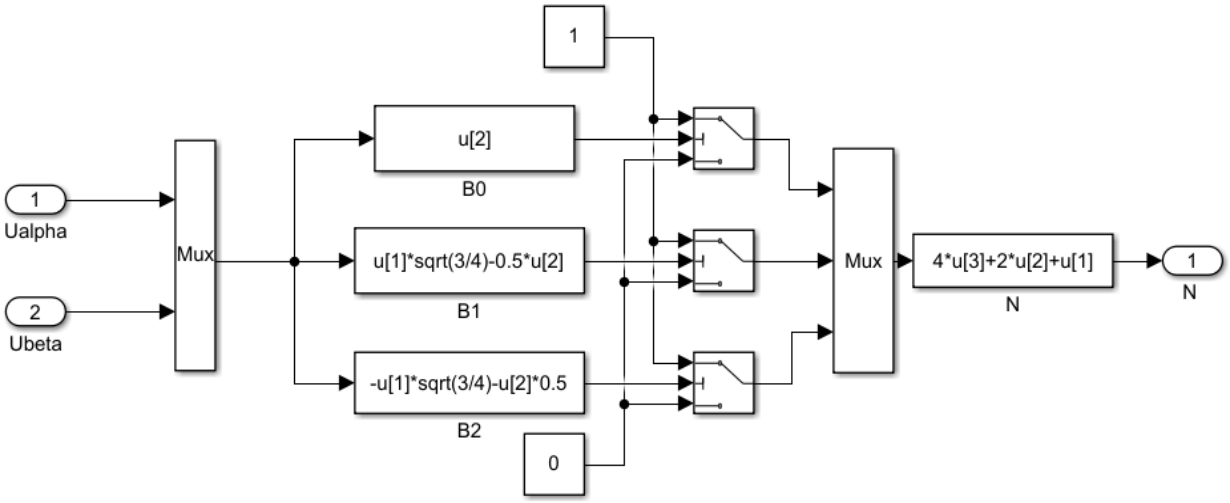

Figure B1.2:

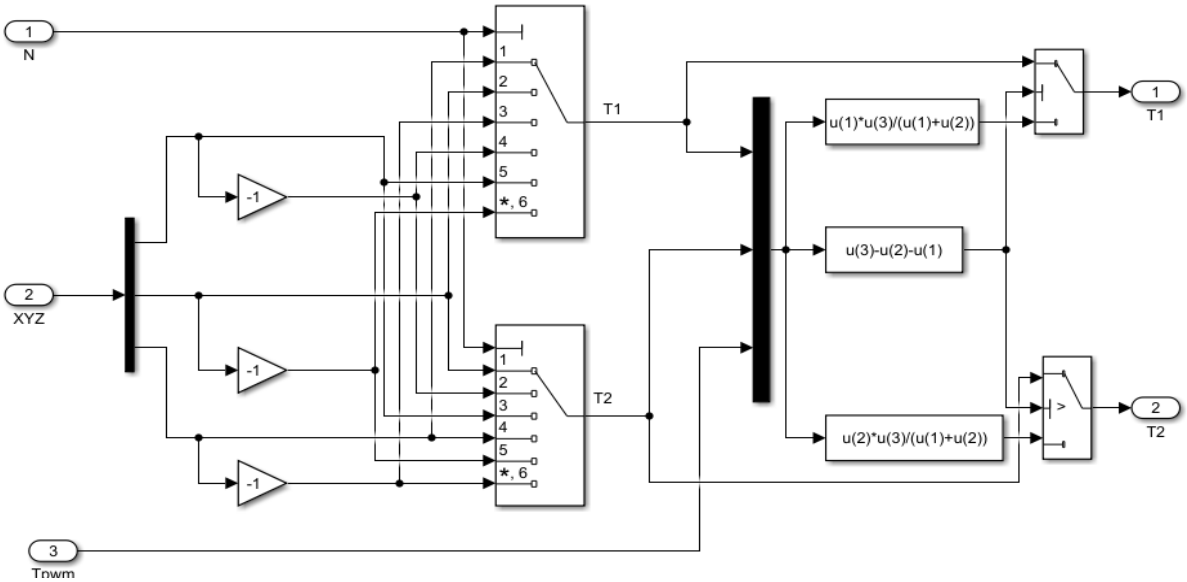

Figure B1.3:

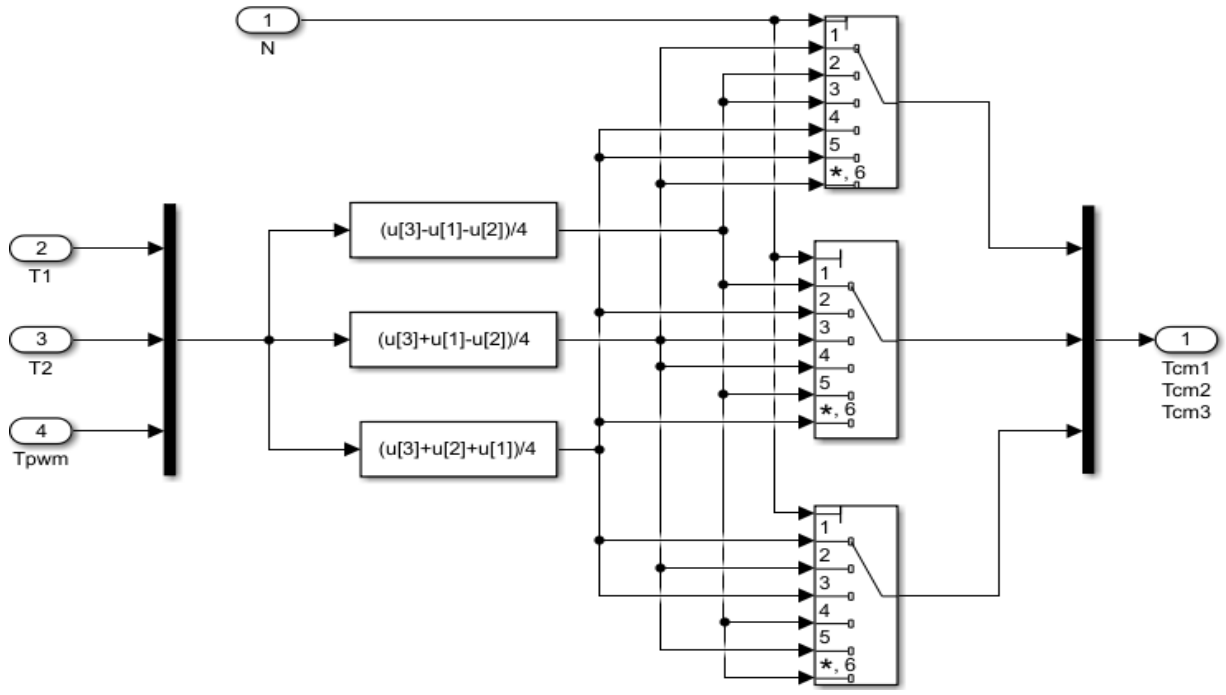
1
N
2
T1
3
T2
4
Tpwm
(u[3]-u[1]-u[2])/4
(u[3]+u[1]-u[2])/4
(u[3]+u[2]+u[1])/4
1
2
3
4
5
*, 6
1
Tcm1
Tcm2
Tcm3

Figure B1.4

APPENDIX - C

Quasi-continuous sliding mode controller block in the simulation function

Quasi-continuous Sliding controller

```
u = -(z2+2*((abs(z1)+(abs(z0))^(2/3))^(-
1/2))*(z1+(abs(z0))^(2/3)*sign(z0)))/(abs(z2)+2*((abs(z1)+(abs(z0))^(2/3))^(1/2)));
if isnan(u)
   u=0;
end
end
```

Differentiator

```
v0 = -14.7361*(abs(z0-s))^(2/3)*sign(z0-s)+z1;
v1 = -30*(abs(z1-v0))^(1/2)*sign(z1-v0)+z2;
z0_d = v0;
z1_d  = v1;
z2_d  = -400*sign(z2-v1);
end
```

Current cost function in high order sliding mode control

```
function iq_r = fcn(e,w)
k  = 20;
del  = 10;
ep  = 0.1;
p  = 4;
J = 0.003;
Si  = 0.175;
B  = 0.008;
an  = 3*p^2*Si/(2*J);
%bn = p/J;
cn = B/J;
eq_s = (k)/(ep+(1+1/(abs(e)))*exp(-del*abs(e)));
iq_r =an^(-1)*(cn*w+(110000+eq_s)*sign(e));
if iq_r<-30
```

```
    iq_r =-30;
end
if iq_r>30
    iq_r = 30;
end
end
```